Available online at www.sciencedirect.com

SCIENCE DIRECT®

Ore Geology Reviews 28 (2006) 308–328

ORE GEOLOGY REVIEWS

www.elsevier.com/locate/oregeorev

Major types, characteristics and geodynamic mechanism of Upper Paleozoic copper deposits in northern Xinjiang, northwestern China

Chunming Han[a,*], Wenjiao Xiao[a], Guochun Zhao[b], Jingwen Mao[c], Sanzhong Li[d], Zhen Yan[a], Qigui Mao[a]

[a] *State Key Laboratory of Lithospheric Evolution, Institute of Geology and Geophysics, Chinese Academy of Sciences, Beijing 100029, P.R. China*

[b] *Department of Earth Sciences, The University of Hong Kong, Pokfulam Road, Hong Kong, China*

[c] *Institute of Mineral Deposits, Chinese Academy of Geological Sciences, 26 Baiwanzhuang Road, Beijing, 100037, P.R. China*

[d] *College of Marine Geosciences, Ocean University of China, Qingdao 266003, Shangdong, P.R. China*

Received 29 April 2004; accepted 20 April 2005
Available online 27 December 2005

Abstract

Syn- and post-orogenic Cu mineralization in the northern Xinjiang Paleozoic accretionary and collisional orogenic belt in northwestern China is of great economic interest. About 40 Cu-bearing deposits have been discovered in the area, making it one of the most important metallogenic belts in China. According to their host rocks, these deposits can be classified into four principal types: (1) volcanic-hosted massive sulfide Cu–Pb–Zn deposits; (2) porphyry Cu–Mo–(Au) deposits; (3) magmatic Cu–Ni sulfide deposits; and (4) Cu–Mo–Au–Ag skarn deposits. Tectonically, the development of these Upper Paleozoic deposits was closely associated with subduction and collision of the ancient Asian Ocean between the Siberian Block and the Tarim Craton. An important metallogenic epoch involving formation of Cu–Pb–Zn-polymetallic deposits formed during southwestern rollback and associated slab-detachment during Devonian time (400–370 Ma). In southern Altay, southwestern-direct rollback and associated slab-detachment occurred during the Devonian (400–370 Ma), in response to later collision at the accreted continetal margin [Xiao, W.J., Windley, B.F., Badarch, G., Sun, S., Li, J.L., Qin, K.Z., Wang, Z.H., 2004b. Palaeozoic accretionary and convergent tectonics of the southern Altaids: implications for the lateral growth of Central Asia. Journal of the Geological Society of London 161, 339–342], during which the Ashele Cu–Pb–Zn and Keketale Pb–Zn deposits formed. Subduction led to the accretion of the Junggar Ocean arc system in the Middle Devonian. In the Lower to Middle Carboniferous, north-dipping subduction beneath the Dananhu arc triggered the emplacement of granitic porphyries in the Tousuquan and Dananhu island arc belt in the east Tianshan, leading to the formation of the Tuwu and Yandong porphyry Cu–Mo–Au–Ag deposits. In the Upper Carboniferous to Lower Permian, large mafic–ultramafic complexes were emplaced during closure of the ancient Tianshan Ocean, resulting in the formation of several magmatic Cu–Ni sulfide deposits, including the Kalatongke Cu–Ni deposits in north Junggar and Cu–Ni sulfide deposits in the Huangshan–Jing'erquan area of east Tianshan Mountains. Also associated with this extensional event were emplacement of voluminous anatectic granitoids and eruption of volcanic rocks, which led to formation of skarn Cu–Mo (Suoerkuduk Cu–Mo deposit) and Cu–Ag deposits (Weiquan Cu–Ag

* Corresponding author. Tel.: +86 10 6200 7917; fax: +86 10 6201 0846.
E-mail address: CM-Han@mail.igcas.ac.cn (C. Han).

0169-1368/$ - see front matter
doi:10.1016/j.oregeorev.2005.04.002

deposit). The tectonic settings, geological features, and temporal and spatial distribution of these different types of Cu deposits reflect, to a great extent, the accretionary and collisional tectonics that occurred between the Siberian Block and Tarim Block.

Keywords: Copper deposits; Metallogenic belts; Tectonic setting; Xinjiang; China

1. Introduction

The Central Asian Orogenic Belt (CAOB) is situated between the Siberian and Sino–Korean–Tarim Cratons and encompasses an immense area, stretching from the Urals in the west, through Kazakhstan, NW China, Mongolia, NE China to the Okhotsk Sea in the Russian far east (Jahn et al., 2004). Since the IGCP-420 project (Continental Growth in the Phanerozoic: Evidence from Central Asia) began in 1997, the CAOB has become a hotspot of geological research and is regarded as the world's largest site of juvenile crustal formation in the Phanerozoic (Windley et al., 2002; Jahn et al., 2004). In the last 5 years, many papers have been published on this orogenic belt. The majority of these papers focus on petrology, structure, geochemistry and isotopic nature of the orogen, but few studies have discussed metallogenic provinces and epochs of the belt and their relationship with generation and evolution of the juvenile continental crust.

Northern Xinjiang (NW China), a complex mosaic of continental fragments, island arcs, and ocean basins, encompasses a key part of the Central Asian Orogenic Belt. Since the 1990s, numerous investigations on metallogenic provinces and epochs have been undertaken through northern Xinjiang and large amounts of data have been collected (e.g., Hu et al., 1986a,b; Ji et al., 1994, 1999; Liu et al., 1996; Chen et al., 1997; Feng et al., 2000a,b; Qin, 2000; Zhang et al., 2000, 2002, 2003, 2004; Rui et al., 2001, 2002a,b; Wang et al., 2001a,b; Chen and Jahn, 2002; Han, 2002; Han et al., 2002; Li and Liu, 2002; Mao et al., 2002, 2003; Qin et al., 2002; Windley et al., 2002; Han and Zhao, 2003; Han et al., 2003; Xiao et al., 2004a,b; Zhou et al., 2004). These investigations have led to the discovery of numerous metal deposits, especially of Cu, in northern Xinjiang. As a consequence, northern Xinjiang has become a large Cu province and has attracted growing interest from the international exploration community (Allen et al., 1992, 1993; Carroll et al., 1995; Allen and Vincent, 1997; Pirajno et al., 1997). These new data enable a better understanding of metallogenesis of Cu and other metal deposits and their relationships with the tectonic evolution of the CAOB. However, most of the documentation of these deposits was reported in the Chinese literature and there have been no comprehensive reviews relating regional geology and tectonics to the distribution of different types of Cu ore deposits in northern Xinjiang, the major segment of the CAOB. The international geological community thus knows little about these deposits. This paper undertakes the first major review of the general geological characteristics of Upper Paleozoic Cu deposits in northern Xinjiang, especially with respect to their alteration, mineralization, geochemistry, metallogenetic timing and associated lithologies and their relations to the Upper Paleozoic tectonic history of northern Xinjiang and the CAOB.

2. General geological setting of northern Xinjiang

Since "terrane" is a general word for tectonostratigraphic units and thus not a suitable term for the first order tectonic division of the vast regions of northern Xinjiang with many complicated tectonic elements, we prefer to use "domain" to describe the first order tectonic divisions, with "sub-domain" as the second rank division. Each sub-domain is composed of various tectonostratigraphic units (Fig. 1). Therefore, northern Xinjiang, encompassing a wide area of the Altay Mountains, Junggar basin and north Tianshan Mountains, consists of the Altay, Junggar and Tianshan domains, each of which is separated from others by regional-scale deep faults (Fig. 1). The major features of these domains are briefly described as follows (Fig. 2).

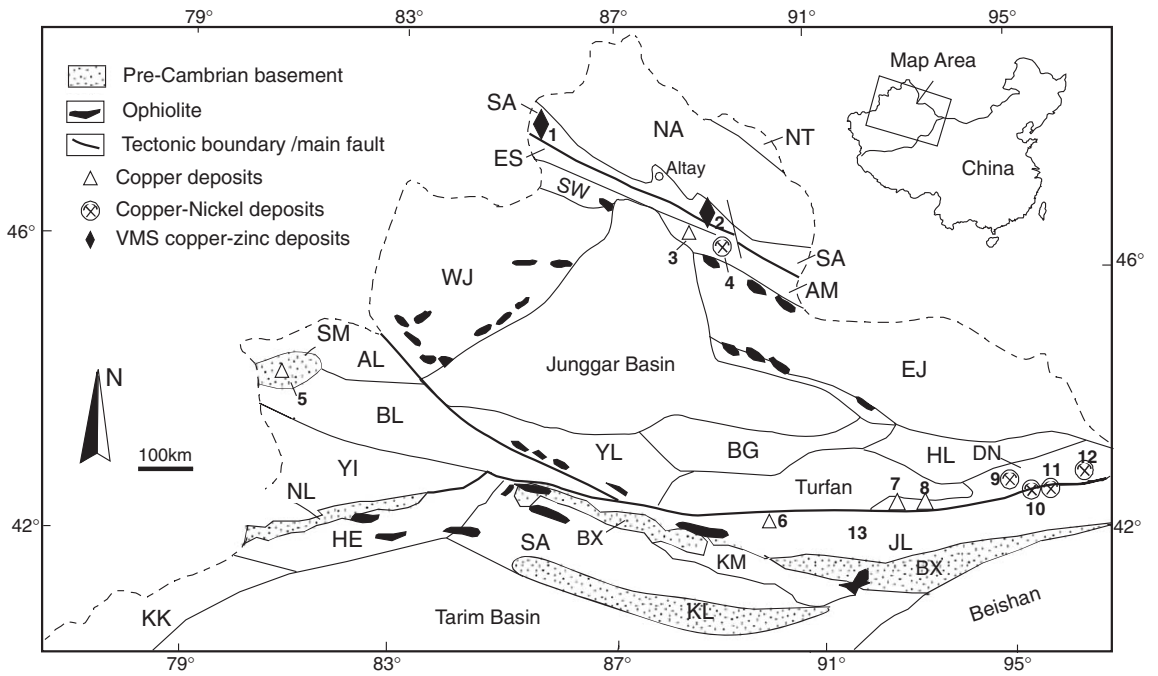

Fig. 1. Sketch map showing the major tectonic units and distribution of copper deposits in north Xinjiang, northwestern China (after Qin et al., 2002). Tectonic units: Altay Domain: NA=Lower Palaeozoic northern Altay tectonic–magmatic belt; NT=Carboniferous–Permian Nuoerte overlapping volcanic basin; SA=Devonian southern Altay magmatic active continental margin; ES=Ertis ductile compression zone; AM=Armantai island arc; and SW=Sawur island arc. Junggar Domain: WJ=western Junggar Sub-domain; EJ=eastern Junggar Sub-domain; BG=Upper Palaeozoic Bogda arc; and YL=Yilianhabierga island arc. East Tianshan Domain: HL=Palaeozoic Harlike island arc; DN=Dananhu–Tousuquan island arc; and JL=Upper Palaeozoic Jueluotag terrane. West Tianshan Domain: YL=Upper Palaeozoic Yilianhabierga back-arc basin; AL=Alatao Paleozoic active margin; BL=Palaeozoic Boluohuoluo island arc; YL=Permian–Carboniferous Yili intracontinential rift; and NL=Nalati–Harlike terrane. Tianshan Domain and affiliated terranes along the Tarim Plate: KL=Pre-Cambrian Kuluketag block; BX=Pre-Cambrian Baluntai–Xingxingxia block; KM=Lower Paleozoic Kumishi block; SA=Upper Palaeozoic Saaerming block; HE=Lower Paleozoic Haerke block; KK=Lower Paleozoic Kuokesaling block; and Beishan=Permian–Carboniferous Beishan aulacogen. Names of ore deposits: 1=Ashele VMS Cu–Zn deposit; 2=Keketale VMS Pb–Zn deposit; 3=Suoerkudouke Cu–Au deposit; 4=Kelatongke Cu–Ni deposit; 5=Lamansu Cu deposit; 6=Xiaorequanzi Cu deposit; 7=Yandong Cu–Mo deposit; 8=Tuwu Cu–Au deposit; 9=Xiangshan Cu–Ni deposit; 10=Huangshan Cu–Ni deposit; 11=Huangshandong Cu–Ni deposit; 12=Hulu Cu–Ni deposit; and 13=Weiquan Cu–Ag deposit.

2.1. Altay domain

Located in the northernmost part of Xinjiang, the Altay Domain extends along the NW-trending Altay Mountains. Its northern, western and southeastern parts extend into Russia, Kazakhstan and Mongolia, respectively, and its southern part is separated from the Junggar Domain by the Irtysh (Erqis) deep fault (Fig. 1). Upper Mesoproterozoic to Lower Cambrian metamorphic rocks form the basement of the Altay Domain, which is overlain by Paleozoic (Ordovician to Silurian) cover that consists predominantly of nearly 10,000 m of marine clastic rocks and intermediate-acid volcanic rocks. The Upper Paleozoic (Devonian) volcanic rocks are a bimodal spilite–keratophyre assemblage, suggesting that they were erupted in an extensional setting (Wang et al., 2002).

Carboniferous magmatism is widespread throughout the Altay Domain and is dominated by calc-alkaline arc magmatism (Rui et al., 2001; Windley et al.,

Fig. 2. Synoptic lithologic diagram of the north Xinjiang (after Li et al., 1998). N=Neogene; E=Paleogene; K=Cretaceous; J=Jurassic; T=Triassic; P=Permian; C=Carboniferous; D=Devonian; S=Silurian; O=Ordovician; ε=Precambrian; Z=Sinian; Pt_3^1=Upper Proterozoic; Pt_2=Mid-Proterozoic; Pt_1=Lower Proterozoic; and Ar=Archaean.

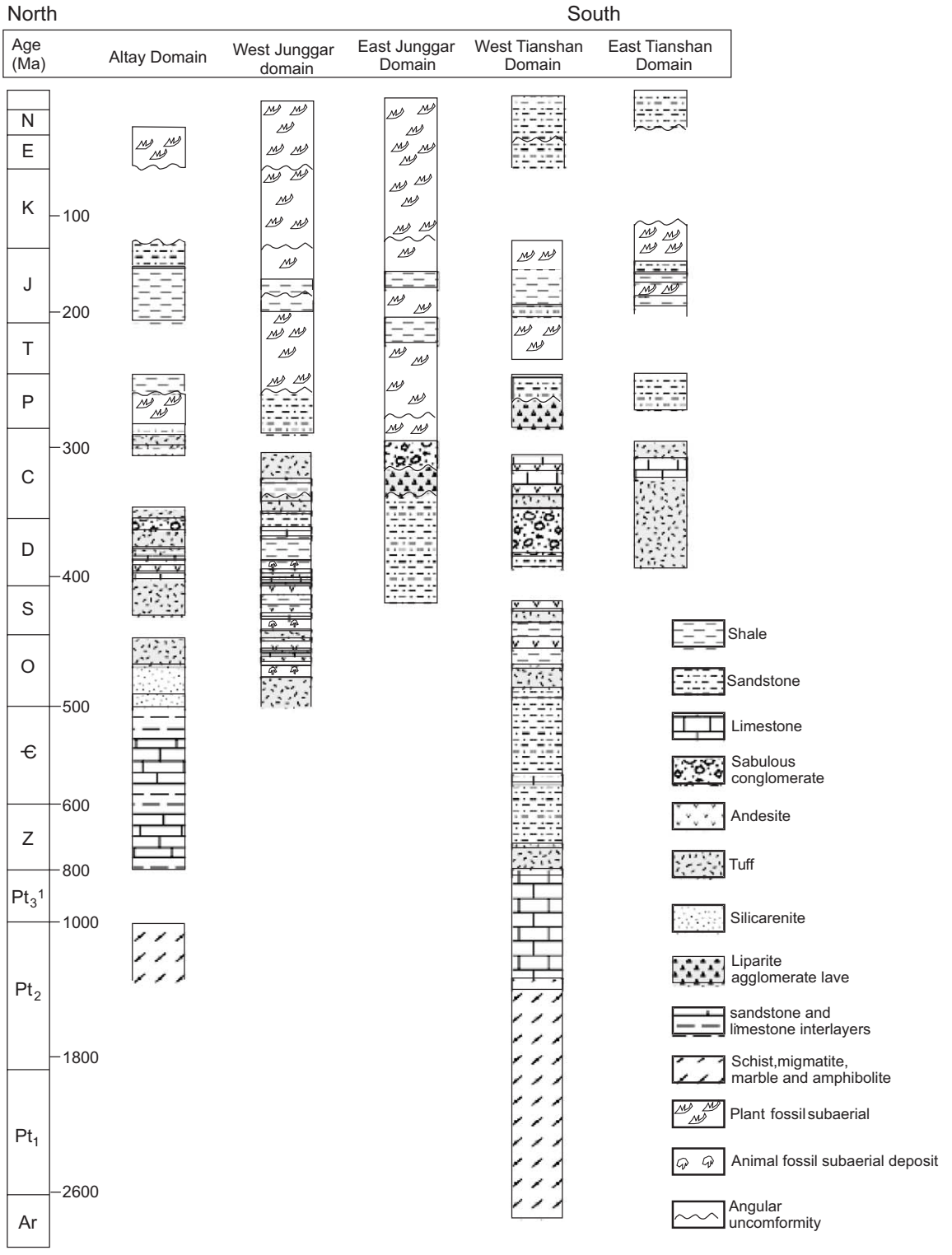
North
South
Age (Ma)
Altay Domain
West Junggar domain
East Junggar Domain
West Tianshan Domain
East Tianshan Domain
N
E
K
J
T
P
C
D
S
O
Є
Z
Pt3 1
Pt2
Pt1
Ar
100
200
300
400
500
600
800
1000
1800
2600
Shale
Sandstone
Limestone
Sabulous conglomerate
Andesite
Tuff
Silicarenite
Liparite agglomerate lave
sandstone and limestone interlayers
Schist,migmatite, marble and amphibolite
Plant fossil subaerial
Animal fossil subaerial deposit
Angular uncomformity

2002). Most of the calc-alkaline magmatism is considered to have resulted from Lower Carboniferous oblique subduction. Upper Carboniferous to Lower Permian post-orogenic right-lateral displacement along many terrane sutures, such as the Irtysh fault, has complicated recognition of the original continental margin (Şengör et al., 1993). Variscan alkaline magmatism north of the Irtysh fault is known for its association with some of the world's largest pegmatite-type rare metal deposits (Rui et al., 2001). Regional metamorphism in the Variscan formed greenschist to amphibolite facies assemblages in Paleozoic rocks, whereas the package of Sinian to Lower Cambrian rocks comprises lower grade slates and phyllites.

2.2. Junggar Basin and eastern and western Junggar Domains

Located between the Altay and Tianshan Terranes, the Junggar Domain extends westward to the Junggar–Balkhash area in Kazakhstan and eastward to southern Mongolia. Traditionally, it has been divided into the Junggar Basin and the eastern and western Junggar Sub-domains.

The Junggar Basin is covered by Cenozoic sediments and Paleozoic and Mesozoic rocks are exposed on the margins of the basin. Controversy has surrounded the age and nature of the basement of the basin for a long time (Gao et al., 1998), with some believing that the basement is a Precambrian microcontinental block (Ren and Jiang, 1980; Wang, 1986; Watson et al., 1987), whereas others interpreted it as Paleozoic oceanic crust (Li et al., 1982; Jiang, 1984). The development of the basin is considered to have been associated with the Upper Permian to Lower Triassic extension (Allen et al., 1995), although some researchers argue that it may not have formed until the Jurassic (Hendrix et al., 1992).

The eastern Junggar Sub-domain comprises several NW–SE trending, highly deformed, metasediments and ophiolite assemblages, which were accreted to the southern margin of the Siberian Plate along the Irtysh deep fault (Fig. 1). The sub-domain is underlain to the east by Upper Devonian to Upper Carboniferous volcanic arc formations and volcanogenic deep marine sedimentary successions. The fault itself probably represents a thrust suture zone between different Paleozoic blocks of the Altaid sequences, which were brought together during the Upper Carboniferous to Lower Permian closure of the Junggar Ocean (Carroll et al., 1995; Xiao et al., 2004a,b). Syn- to post-kinematic, felsic to intermediate granitoids are scattered on both sides of the fault and chromite-bearing ultramafic bodies occur along the fault zone. These bodies are poorly studied, although a variety of granitoids have K–Ar and Rb–Sr dates ranging between about 360 and 230 Ma (Chen, 1999). Granitoid rocks were emplaced in the eastern Junggar Sub-domain (Hu et al., 2000), with a major period of intrusion in the Upper Paleozoic (320–250 Ma; Lu and Liu, 1989; Zhou, 1989; Hu et al., 2000). They range in composition from I-type calc-alkaline to A-type alkaline granitoids (Chen and Jahn, 2004). The mafic/ultramafic rocks occur mainly in the northern part of the eastern Junggar sub-domain, represented by the Cu–Ni-bearing Kalatonke plutons, which have a Sm–Nd isochron age of 298 ± 11 Ma, interpreted as the age of the extensional event that led to the emplacement of basic/ultrabasic rocks (Li et al., 1998). Huang et al. (1997) obtained Sm–Nd isochron age of 561 ± 41 Ma for the gabbros, diabases, andesites and porphyrites from the Armantai ophiolites.

The western Junggar Sub-domain was accreted to the Kazakhstan Plate to the west, with the Darabut and Saur strike–slip faults as the major suture zones between them. The western Junggar Sub-domain is characterized by the Devonian to Lower Carboniferous metasedimentary rocks, oceanic basalts, formed in ophiolitic sequences, and some mélanges (Shen et al., 1996). Although the rock types and ages of the western Junggar Sub-domain are similar to those of the northern Altaids, lithologies and major fault zones trend NE–SW in the western Junggar Sub-domain are almost orthogonal to those of the Altaids (Rui et al., 2001). Ophiolites from the western Junggar Sub-domain have been geochronologically dated, particularly using Sm–Nd isochron methodology (Hu et al., 2000). Some published results are summarized as follows (Zhang and Huang, 1992; Huang et al., 1995; Hu et al., 2000): (1) the Tangbale ophiolites yield Sm–Nd isochron ages of 489 ± 53 and 447 ± 56 Ma for gabbros and basalts, respectively; (2) the Honggule-leng ophiolites yield a Sm–Nd isochron age of 625 ± 25 Ma for gabbros, diabases, olivine syenites, augite anorthosites and plagioclases (Huang et al., 1995); and (3) the Dalabute ophiolites yield a Sm–Nd isochron age of 395 ± 12 Ma for gabbros. These

isotopic results do not support the presence of Precambrian basement in the Junggar Sub-domains (Hu et al., 2000).

2.3. East and west Tianshan Sub-domains

The Tianshan Domain is a complex orogen with composite terranes and doubly sutured belts (Windley et al., 1990; Xiao et al., 1992; Hu et al., 2000). The eastern part of this >2500-km-long mountain belt trends E–W across a 300-km-wide zone in the center of Xinjiang (Rui et al., 2002a; Han and Zhao, 2003). Tectonically, the Tianshan Range can be divided, from north to south, into the northern, central and southern Tianshan.

The western Tianshan Sub-domain consists of the following lithologic groups (Bureau of Geology and Mineral Resources of Xinjiang Uygur Autonomous Region, 1993; Hu et al., 2000): (1) the Nalati Group, composed of hornblende–plagioclase gneiss, migmatite, and minor greenschist, quartzite and dolomitic marble; (2) the Muzha'erte Group, composed of granitic gneisses, leptynite, marbles, and fine-grained metasediments; and (3) the Wenquan Group, made up of amphibolites, amphibole–quartz schists, banded and augen gneisses, migmatite, mica schists and marbles.

The east Tianshan Sub-domain mainly comprises the Devonian, Carboniferous and Permian stratigraphic sequences. The Devonian strata can be further divided into the lower, middle and upper sequences. The Lower Devonian sequence is called the Danhu Formation that is composed of tholeiite, andesite, lithic sandstone, tuff, siltstone and lithic arkose (He et al., 1994). The Middle to Upper Devonian sequences, named the Tousuquan Formation, consist predominantly of tholeiite, tuff, felsite, andesite, trachyandesite, quartz andesite and dacite (He et al., 1994). Carboniferous rocks in the eastern Tianshan Sub-domain have also been divided into lower, middle and upper sequences, of which the Lower Carboniferous includes the Xioarequanzi, Yanmansu, Gandun and Wutongwozi Formations (He et al., 1994; Ma et al., 1997).

Granitic rocks are widely intruded in the eastern and western Tianshan Sub-domains and are mostly Upper Paleozoic in age (~300 Ma), but minor granites were emplaced in the Lower Paleozoic (400~450 Ma; Hu et al., 2000) or Neoproterozoic (1200~960 Ma; Hu et al., 1986a).

3. Types of Cu–(Ni) deposits and their major characteristics

Copper–(nickel) deposits in northern Xinjiang have been assigned to four major types according to the tectonic setting in which they formed. These are: (1) pre-accretionary Devonian volcanic-hosted Cu–Pb–Zn massive sulfide deposits, (2) syn-accretionary Lower Carboniferous porphyry-type Cu–Mo–(Au) deposits, (3) syn-to post-accretionary Upper Carboniferous–Lower Permian magmatic Cu–Ni–sulfide deposits; and (4) post-accretionary Upper Carboniferous–Lower Permian skarn Cu–Mo–Au–Ag deposits. The main characteristics of these four types of Cu deposits are listed in Table 1 and are summarized as follows.

3.1. Devonian syn-accretionary volcanic-hosted Cu–Pb–Zn massive sulfide deposits

Deposits that are hosted in marine volcanic rocks and contain a substantial amount of pyrite and a certain quantity of Cu, Pb and Zn sulfide ores are called volcanogenic massive sulfide (VMS) Cu–Pb–Zn deposits. Based on the metallic element associations and metallogenic tectonic environments, this type of deposits can be further divided into two: Cu–Zn and Zn–Pb–Cu Groups. VMS deposits in the first group are hosted by sequences dominated by mafic volcanic rocks and are particularly abundant in Archean and Early Proterozoic greenstone belts, whereas those in the latter group are hosted by sequences dominated by Phanerozoic felsic volcanic rocks and best exemplified by Kuroko deposits of the Miocene Green Tuff Belt of Japan. The Cu–Zn group can be further subdivided into four types: (1) Noranda-type: hosted in mafic–felsic volcanic sequences in the Archean and Palaeoproterozoic greenstone belts; (2) Mattabi-type: similar to the Noranda-type but containing more Pb and Ag, and much higher proportion of felsic volcanic rocks in the footwall; (3) Cyprus-type: hosted by ophiolites; considered to be the most convincing ancient analogs of sea-floor sulfide deposition; and (4) Besshi (Ural)-type: hosted by sediments in volcanic terranes (Wang et al., 1998). VMS deposits in northern Xinjiang correspond to the Besshi-type. They occur in an extensional environment and are hosted by typical bimodal volcanic assemblages (He et al., 1994).

Table 1
Summary of types and main characteristics of the copper deposits in northern Xinjiang

Typical deposits (long., lat.)	Genetic types	Main metals	Reserve	Ore minerals	Wall-rock alteration	References
Ashele (86°18′45″ E, 48°15′16″ N)	VHMS	Cu–Pb–Zn	1.08 Mt Cu, 10 t Au, 860 t Ag	Chalcopyrite, pyrite, sphalerite, galena, tennantite, argentite, bornite, cubanite	Silicification, sericitization, pyritization, chloritization, carbonatization	Chen et al. (1996), Li et al. (1998), Wang (1996)
Keketale (89°11′54″ E, 47°21′10″ N)	VHMS	Pb–Zn	3 Mt Pb+Zn	Pyrite, pyrrhotite, magnetite, galena and sphalerite, arsenopyrite, chalcopyrite, tetrahedrite, bornite and marcasite	Silicification, sericitization, carbonatization, chloritization, epidotization, pyritization	Chen et al. (1996), Li et al. (1998), Wang et al. (1998)
Tuwu (92°37′ E, 42°07′ N)	Porphyry	Cu–Mo–Au	0.99 Mt Cu, 19.4 t Au 419 t Ag	Chalcopyrite, pyrite, bornite, chalcocite, molybdenite	Silicification, chloritization, albilization, sericitization, epidotization,	Rui et al. (2001), Wang et al. (2001a), Qin (2000), Han et al. (2003)
Kalatongke (89°40′35″ E, 46°45′27″ N)	Magmatic Cu–Ni	Cu–Ni–PGE	No.1 orebody: 38.6 Mt Cu+Ni, No.2 and No.3 orebody: 28.4 Mt Cu+Ni	Pyrrhotite, chalcopyrite, pentlandite, violarite, magnetite	Sericitization, chloritization, carbonatization, silicification	Li et al. (1998), Wang and Zhao (1991), Yan et al. (2003)
Huangshan (94°36′00″ E, 42°16′46″ N)	Magmatic Cu–Ni	Cu–Ni–PGE	0.21 Mt Cu, 0.32 Mt Ni	Pyrrhotite, pentlandite, chalcopyrite, violarite, mackinawite	Serpentinization, uralitization, talcigation, chloritization, carbonatization	Li et al. (1998), Li and Li (1991)
Huangshandong (94°43′12″ E, 42°17′48″ N)	Magmatic Cu–Ni	Cu–Ni–PGE	0.18 Mt Cu, 0.36 Mt Ni	Pyrrhotite,.pentlandite and chalcopyrite, with subordinate pyrite, cobalt pyrite, violarite, cubanite, mackinawite, millerite, arsenopyrite, marcasite	Serpentinization, talcigation, chloritization, amphibolization	Li et al. (1998), Li and Li (1991), Mao et al. (2002), Mao et al. (2003)
Lamasu (80°44′00″ E, 44°15′00″ N)	Skarn Cu deposit	Ag–Cu	No data	Chalcopyrite, molybdenite, pyrite, pyrrhotite	K-feldspathization, albitization, sericitization, chloritization, silicification	Li et al. (1998)
Suoerkudouke (88°45′22″ E, 46°44′51″ N)	Skarn Cu–Mo deposit	Cu–Mo–Au–Ag	244,160 t Cu, 12,102 t Mo, 5.11 t Au, 194 t Ag	Chalcopyrite, pyrite, sphalerite, galena, molybdenite, marcasite, pyrrhotite, calaverite	Skarnification, chloritization, epidotization, serpentinization	Li et al. (1998)
Weiquan (91°43′47″ E, 41°52′18″ N)	Skarn Ag-Cu deposit	Ag–Cu	59,516 t Cu, 1272 t Ag	Chalcopyrite, pyrite, galena, sphalerite, molybdenite	Skarnification, chloritization, epidotization, serpentinization	Han (2002), Han et al. (2002), Wang et al. (2001a,b)

The oldest important mineral deposits recognized in northern Xinjiang are the polymetallic VMS deposits, including Ashele and Keketale, the largest deposits. They are almost entirely restricted to a NW-trending belt of rocks, >360-km-long by 30–70-km-wide, made up of the Lower Devonian Kangbutiebao and Ahsele Formations. More Cu-rich massive sulfides are hosted by the mafic volcanic rocks. These deposits are quite common in accreted arcs within Phanerozoic Cordilleran-style orogens and are well recognized in the accreted terranes of both California and southern Alaska (Goldfarb et al., 2003).

3.1.1. Ashele Cu–Pb–Zn deposit, Habahe County, Altay

The Ashele Cu–Pb–Zn deposit, a typical VMS deposit, was discovered during a regional geological survey in 1984. The deposit is located 30 km northwest of Habahe City. Tectonically, it is located in the Lower Paleozoic Altay tectonomagmatic belt of the Siberian Block (Fig. 1). It is separated to the southwest from the Altay ore district of the former USSR by the Marka Kol fault.

The main strata exposed in the ore district are the Middle Devonian Altay Formation and Middle to Upper Devonian Qiye Formation. Structures in the ore district are controlled mainly by a number of N–S-trending folds and faults, with the structural line extending from south to north. The faults are mainly post-ore ones and mainly strike NW and N–S. Generally, volcanic edifices form at the intersections of two sets of faults. Orebodies are hosted mainly in tuff and breccias in the second succession of the Altay Formation, with basalt and quartz keratophyre as the hanging walls. Seven mineralization zones are distributed along the N–S-trending faults in the ore district. The length of each individual mineralization zone ranges from several meters to several hundreds of meters, with a maximum length up to 1 km and a general width up to tens of meters. Sulfide orebodies of different sizes are distributed in all zones, of which orebody No. 1 is the largest and is the main orebody in the district. Orebody No. 1 is a lens-shaped mound concordant with bedding and folded synchronously with the strata. Close to the main orebody are a number of small vein-type orebodies. The main orebody strikes N–S and dips E at an angle of 50° and extends 500 m in length and up to 1000 m vertically. The thickness of the orebody ranges from 5 to 50 m, with the maximum thickness of ~180 m in the axial zone of a syncline. The ores exhibit massive, densely disseminated, banded, veinlet-disseminated, and brecciated structures. The orebody shows pronounced vertical zoning, with its lower part consisting of veined and veinlet-disseminated ores and the middle and upper parts composed of massive ores. From the center of the orebody toward edges, the ores grade from massive, through banded, to disseminated structures. The dominant ore component is Cu and the associated components include Zn, Ag, Pb, pyrite and barite, with minor Au, Se, Cd, Te and Ga. The ore has an average Cu grade of 3.04% with parts of it over 4%. Associated Zn has an average grade of 3% (Chen et al., 1996).

The Rb–Sr isochron age of ores is 364 ± 15 Ma and the Sm–Nd and Rb–Sr isochron ages of the ferruginous jasper rock of the footwall of the orebody are 373 ± 14 and 378.3 ± 39 Ma, respectively, suggesting that the deposit formed in the Lower–Middle Devonian (Li et al., 1998).

3.1.2. Keketale Pb–Zn–(Ag) deposit

Located ~95 km SE of Altay City, the Keketale Pb–Zn deposit is situated in the Klan rift zone on the Lower–Upper Paleozoic continental margin of the Siberian Block. The strata exposed in the ore district are the Lower Devonian Kangbutiebao Formation, which can be further divided into the lower and upper successions. The lower succession consists of intermediate-acid volcanic rocks, pyroclastic rocks and terrigenous clastic rocks and the upper succession comprises intermediate-acid volcanic rocks with intermediate-basic volcanic rocks, terrigenous clastic rocks and appreciable quantities of carbonate rocks. The deposit is located in the second sequence of the upper succession of the Kangbutiebao Formation. A large number of faults have been recognized in the orefield, with WNW-trending compressional faults predominating. The major fold structure in the area is represented by the Maizi composite overturned syncline.

Magmatic rocks in the orefield are dominated by the Middle Hercynian granites. Early Hercynian intermediate-basic intrusions mostly occur as dikes and stocks near the fault zone. Quartz-albite porphyry

and quartz porphyry intrusions are observed as dikes and apophyses in the area of the orefield.

Gangue minerals are quartz, plagioclase, muscovite, calcite, diopside, tremolite, almandine, biotite, hornblende and epidote. The ores have finely granular, corroded and interstitial textures and disseminated, mottled and massive structures with less common banded, laminated, stockwork and brecciated structures. Lead grade in the orebodies is 0.38 to 4.95%, with a mean of 1.51%; Zn grade is 0.40 to 10.74%, with a mean of 3.16%; and the mean grade of Pb + Zn is 4.67%. The Ag grade is commonly <40 g/t, with the highest grade of 222 g/t. According to the mineral assemblages, Wang et al. (1998) divided the mineralization into two stages: the early stage characterized by the pyrrhotite+pyrite+sphalerite+galena mineralization and the late stage by the occurrence of pyrite + galena ore veins.

Sphalerite in the ores gives a Sm–Nd isochron age of 373 ± 15 Ma and disseminated Pb–Zn ores yield a Rb–Sr isochron age of 273.6 ± 7.5 Ma (Li et al., 1998). The former represents the mineralization age of the Keketale Pb–Zn deposit, whereas the latter represents a late thermal event.

3.2. Upper Devonian–Lower Carboniferous syn-accretionary porphyry Cu deposits

Porphyry Cu deposits mainly occurred in the middle of highly mineralized Devonian and Lower Carboniferous accreted volcanic island arcs and, from west to east, they are the Yandong, Tuwu, Linlong, Chihu and Yaziquan deposits (Han et al., 2003), of which the most representative is the Tuwu Cu deposit, the major features of which are as follows.

The Tuwu deposit is hosted in the Carboniferous Qi'eshan Group of the Dananhu–Tousuquan island arc. The country rocks in the arc consist of basalt, andesite, spilite, keratophyre, andesitic brecciated lavas, lithic sandstone, pebbly lithic sandstone, polymictic conglomerate and sedimentary tuff. The strata, generally with well-developed schistosity, strike nearly E–W direction and dip south at 43–63°.

The Cu grade of the ore is generally 0.30–1.5%. The Cu orebody, delineated using the cut-off grade of 0.5%, has an average Cu grade of 0.72%; average Au and Ag grades are 0.16 and 2.97 g/t, respectively. The dominant ore minerals are chalcopyrite, bornite and pyrite (Table 1); the main gangue minerals are quartz, plagioclase, sericite, chlorite and biotite, with minor hornblende, pyroxene, epidote, zoisite and calcite. Secondary alteration minerals are malachite and limonite.

Based on crosscutting relationships, the Tuwu Cu deposit can be divided into six mineralization stages. Stage 1 represents the stage of the independent volatile phase (dominated by magmatic water) and is characterized by Mg-rich biotite accompanied by albite and K-feldspar. In this stage, a part of the metal sulfides were deposited and a chalcopyrite+bornite+-pyrite assemblage is observed in biotite-rich spots and veinlets. Stage 2 is characterized by the phyllic alteration and quartz+pyrite+chalcopyrite veins. The stage 3 mineral assemblage is quartz+vein molybdenite. The stage 4 mineral assemblage consists of sulfates (gypsum+anhydrite), with some sulfide veinlets. Stage 5 is characterized by the presence of carbonate (calcite)+laumontite+minor sulfides. Stage 6 is characterized by supergene oxidation, which led to the development of secondary minerals, malachite and limonite.

Rui et al. (2002b) obtained a Re–Os molybdenite isochron age of 323 ± 2.3 Ma from the Tuwu porphyry Cu deposit. The same authors also carried out zircon U–Pb SHRIMP dating of mineralized basic volcanic rocks and obtained mineralization and alteration ages ranging from 308 ± 6.1 to 344.3 ± 6.8 Ma, with a mean of 320.1 ± 7.7 Ma. Qin (2000) used the K–Ar and $^{40}Ar/^{39}Ar$ methods to determine the ages of sericite and quartz from two ore-bearing porphyries of Tuwu and Yandong (311.1 ± 4.6 and 341.2 ± 4.9 Ma, respectively. Liu et al. (2003) performed ion probe (SHRIMP) microanalysis on differently shaped zircon crystals from ore-bearing plagiogranite–porphyries at the Tuwu–Yandong Cu deposit. The analytical results show that the weighted mean age of 16 zircon grains from the Tuwu Cu deposit is 333 ± 2 Ma (95% confidence level). From the above-mentioned age data we conclude that the mineralization age of the Tuwu Cu deposit is between 340 and 310 Ma.

3.3. Upper Carboniferous–Lower Permian syn- to post-accretionary magmatic Cu- and Ni-deposits

The host rocks of this type of deposit are mainly late Variscan mafic–ultramafic rocks and distributed

in northern Junggar and Huangshan–Jing'erquan areas in the eastern part of east Tianshan. The major deposits are the Kalatongke, Huangshan and Huangshandong deposits. Copper–nickel deposits in (Kalatongke and Huangshan) are mostly of magmatic origin and occur in those orogenic belts that are far from cratonic blocks. Their tectonic environments are different from those of the same type of deposits in other areas of China (e.g., the Jinchuan deposit Gansu Province and the Limahe deposit, and Sichuan Province) and the world (Noril'sk, Russia and Sudbury, Canada). The mineralized intrusions of the Jinchuan and Sudbury deposits are both Mesoproterozoic in age and are constrained by deep faults on continental margins of the north China Craton and eastern Canadian Craton, respectively, but they are different in that the mineralized basic complex of the Sudbury deposit occurs as a lopolith, whereas the mineralized intrusion of Jinchuan occurs as a small stock. The Limahe and Noril'sk deposits occur on the southwestern margin of the Yangtze Craton and on the northwestern margin of the Siberian Craton, respectively; both are also controlled by the old cratons. At present no Cu–Ni sulfide deposits of great commercial value have been found in the Phanerozoic cratons. Therefore, the mineralization of Cu–Ni sulfide deposits in northern Xinjiang has unique characteristics.

3.3.1. Kalatongke Cu–Ni deposit

The Kalatongke Cu–Ni deposit, found in 1978 (Yan et al., 2003), is located in an island arc belt of the Altay orogenic belt, at the southern margin of the Siberian Plate (Fig. 1), bounded by the NW-trending Irtysh and Ulungur deep faults. The strata exposed in the ore district are mainly the Middle Devonian Yundukala Formation and Lower Carboniferous Nanmingshui Formation. The orefield is located in the eastern segment of the Sarbulak synclinorium. The latter, with a NW-striking axis, is composed of a number of NW- and NNW-trending folds. Fault structures are well developed in the district and may be divided, on the basis of strike, into NW, NNW, EW and NE sets, of which the NW and NNW sets are the ore-controlling structures in the district.

Mafic–ultramafic intrusions, which occur along the NW-trending fault belts and are emplaced within the Lower Carboniferous Nanmingshui Formation, are exposed in ore district 11. The intrusions strike NW, parallel to the lineament. The Cu–Ni orebodies of the Kalatongke deposit are mainly hosted in a mafic–ultramafic intrusion of the northern belt. Of these, intrusion No. I contains the most significant mineralization—a body 695 m long and a maximum of 160 m wide, with an exposed area of ~0.1 km^2, striking 330° and dipping E, with the upper part dipping at 70–90° and the lower part at 0–60°. Intrusion No. I may be further divided into diabase–gabbro, olivine–norite, norite and diorite zones, which exhibit gradational relationships and are pervasively mineralized. The mineralization occurs in olivine norite, norite and a lesser amount in diabase–gabbro. The rocks are Mg-rich and Ca-poor and the Mg/Fe ratio is about 1.33 in the upper part, ~1.59 at the base, ~2.55 in the middle-upper part, and ~2.45 in the middle-lower part. The orebody is composed of disseminated ores and massive primary sulfide ores. Ore textures include drop-like disseminations, massive, banded, and veinlet-stockwork structures and sideronitic types. In the massive ores, Ni and Cu contents range from 3.1% to 4.55% and 2.12% to 9.73%, respectively; in the intermediately to densely disseminated ores, Ni and Cu contents are 0.87% and 1.15%.

Wang and Zhao (1991) used the Rb–Sr isochron method to determine ages of olivine norite, norite, hybrid norite and diabase–gabbro in the Kalatongke intrusion at 285 ± 16, 298 ± 23, 302 ± 32 and 317 ± 50 Ma, respectively. Li et al. (1998) applied the Sm–Nd method to biotite–hornblende–olivine norite, plagioclase harzburgite and diorite from the same intrusion and obtained an isochron age of 297.7 ± 11 Ma, which is in agreement with the Rb–Sr isochron ages obtained by Wang and Zhao (1991). It is thus inferred that the emplacement age of the Kalatongke intrusion is between 298 and 285 Ma. In addition, massive and densely disseminated sulfide ores of the Cu–Ni deposit in the Kalatongke intrusion yield a Sm–Nd isochron age of 281 ± 12 Ma (Li et al., 1998). This result is essentially consistent with the emplacement age of this intrusion, indicating that petrogenesis and mineralization of the Kalatongke intrusion took place essentially simultaneously.

3.3.2. Huangshan Cu–Ni sulfide deposit

The Huangshan (Huangshanxi) Cu–Ni sulfide deposit is situated 140 km southeast of Hami City, Xinjiang and is located in the Dananhu–Tousuquan

island arc belt of the Kazakhstan–Junggar Block (Fig. 1). The deposit lies in the western part of the Huangshan–Jing'erquan basic–ultrabasic belt SE of Hami City. The strata exposed in the ore district are the Lower Carboniferous Gandun Formation, which can be subdivided into five lithological units. The Huangshan complex was emplaced near the axial zone of the Gandun anticlinorium, controlled by the NNE-trending Kangurtag deep fault and its secondary faults.

Magmatic rocks of the region include granites and basic–ultrabasic rocks. Granites are mainly distributed in the southwestern and eastern parts of the orefield and include three intrusions. No. III diorite intrusion, in the SW part of the orefield, is 600 m long and 30–50 m wide, extends in a nearly E–W direction, and contains no indication of Cu–Ni mineralization. No. II intrusion consists of websterite, gabbro–norite and gabbro and is in the eastern part of the orefield. It is 1900 m long, 100–150 m wide, and elongated in an ENE–WSW direction. Deep drilling has verified that there are Cu–Ni ores present. No. I intrusion stretches across the central part of the orefield, extending 3950 m E–W, and is on average 400 m wide. The intrusion consists of a series of dikes of complex character, formed by intrusion of basic–ultrabasic magmas of different phases. Three mineralization zones have been recognized on the surface. Deep drilling has also revealed that the Cu–Ni sulfide orebodies are intimately associated with mafic–ultramafic rocks.

The whole-rock Sm–Nd age is 308.9 ± 10.7 Ma, the ore Sm–Nd age is 305.4 ± 2.4 Ma (Li et al., 1998), and the whole-rock Rb–Sr isochron age is 280 Ma (Li and Li, 1991). Recently, Zhou et al. (2004) obtained a SHRIMP U–Pb zircon age of 269 ± 2 Ma from igneous zircons separated from a diorite in the Huangshan intrusion. It is suggested that the ages of emplacement and mineralization are Upper Carboniferous to Lower Permian.

3.4. Post-accretionary Upper Carboniferous–Lower Permian skarn deposits

Skarn-type Cu deposits are found in the contact zone (skarn zone) between intermediate-acid intrusive rocks and carbonate rocks. Skarn-type Cu deposits are typified by the Weiquan Cu–Ag deposit in Shanshan County and other similar deposits found in the contact zone between subvolcanic (andesite–porphyrite) and volcanic and pyroclastic rocks. Generally, the mineralization is restricted to bedded skarn, as exemplified by the Suoerkudouke Cu–Mo deposit in Fuyun County.

3.4.1. Suoerkudouke Cu–Mo deposit

The deposit is situated in the Armantai island arc belt on the southern side of the Irtysh fault belt in the Middle Devonian Beitashan Formation (Fig. 1). The fold structure in the ore district is represented by the Suoerkudouke anticline, which is 9.5 km long, 4.5 km wide, strikes 310° and dips 230° at 30–50°. This anticline controls the Cu–Mo mineralization and spatial localization of orebodies. Faults are well developed in the ore district and strike NW and dip NE. Magmatic rocks in the area are dominantly Middle Hercynian augite diorites. Orebodies are hosted mainly in tuffs in the exocontact zone of augite diorite and augite diorite itself also contains Cu–Mo mineralization.

The orebodies are concordant with the bedding of the strata and concentrate in the central part of the ore district, with the main orebodies occurring in epidote–garnet and garnet–epidote skarns. The ore zone is 2550 m long, 900 m wide, and strikes 330–350° and dips SW at angles varying between 30° and 40°. The principal gangue minerals are epidote, garnet, pyroxene, actinolite, calcite, chlorite, plagioclase, biotite, quartz, diopside and carbonates. The ores have anhedral microgranular, anhedral unequigranular and interseptal textures and disseminated, veinlet-disseminated and veinlet structures. Li et al. (1998) carried out Sm–Nd dating on garnet and epidote in ore-bearing garnet skarn and ore-bearing epidote skarn in the deposit and obtained an isochron age of 284.3 ± 3.9 Ma, indicating that this deposit formed in Lower Permian time.

3.4.2. Weiquan Cu–Ag deposit

The Weiquan deposit is located ~158 km SE of Shanshan city. Tectonically, the deposit is situated in the Carboniferous Aqishan–Yamansu volcanic back arc basin on the northern margin of the Tarim Craton, ca. 3 km north of the Yamansu fault. The strata exposed in the ore district are the Middle Carboniferous Tugutubulak Formation, consisting of siliceous, calcareous pebbly sandstone and pyroclastic rocks

with small amount of limestone; the strata dip south at 44–64°. Intrusive rocks, including diorite, diorite porphyry and albite porphyry, are mainly exposed on the southern side of the orebodies and form dikes and irregular bodies. Carboniferous granite is exposed 3–5 km SW of the ore district. A ring-shaped skarn zone surrounds the intrusion; this intrusion is likely to have provided heat and metals for deposits throughout the ore district.

Ore minerals are chalcopyrite, with subordinate chalcocite, sphalerite and magnetite; Cu-minerals are anhedral, irregularly granular in shape. The principal gangue minerals are quartz, plagioclase, sericite, andradite, chlorite and biotite with minor hornblende, pyroxene, epidote and calcite. Ar–Ar dating of hornblende from diorite yielded an isochron age of 275.8 ± 2.8 Ma, suggesting that this deposit formed in the Lower Permian.

4. Discussion

4.1. Timing of copper mineralization

A large number of isotopic age data are available for Cu–(Ni) deposits in northern Xinjiang. The majority is whole-rock K–Ar or Rb–Sr ages; only a few are Re–Os and Ar–Ar ages (Table 2).

Jaspers in the Ashele Formation yield a Rb–Sr isochron age of 378.3 ± 39 Ma and a Sm–Nd isochron age of 372.7 ± 14.3 Ma, indicating a Middle Devonian age (Li et al., 1998). Dacitic porphyries produced a Rb–Sr isochron age of 294 ± 38 Ma, laminated Cu ores gave a Rb–Sr isochron age of 364–367 Ma, massive ores yielded a Rb–Sr age of 265 ± 8 Ma and an Sm–Nd isochron age of 281.5 ± 10.8 Ma (Li et al., 1998; Wang et al., 2002), and pyrite quartz veins have a Rb–Sr isochron age of 302 ± 11 Ma. On the other hand, tetrahedrite-bearing carbonate–quartz veins have a Rb–Sr isochron age of 255 ± 16 Ma, indicating an Upper Permian age (Li et al., 1998; Wang et al., 2002). Therefore, the Ashele VMS Cu–Pb–Zn deposit may have undergone a protracted mineralization history, although the main phase of mineralization took place in the Devonian. Regional tectonomagmatic activity in the Carboniferous–Permian may have hydrothermally modified and upgraded the deposit.

Copper–nickel sulfide deposits in northern Xinjiang are mainly distributed in the Kalatongke area of northern Junggar and the Huangshan–Jing'erquan area of eastern Tianshan. The Kalatongke intrusion gave Rb–Sr isochron ages ranging from 317 to 285 Ma and K–Ar ages ranging from 209 to 340 Ma. Based on Sm–Nd isotopic data, Li et al. (1998) suggested that the rock- and ore-forming ages of the Kalatongke, Huangshan and Huangshan East ore-hosting intrusions are 297–281, 320–314 and 308–305 Ma, respectively. Qin (2000) obtained a single-grain zircon U–Pb age of 285 ± 20 Ma for the Xiangshan hornblende gabbro. Mao et al. (2002) carried out Re–Os dating on Cu–Ni sulfide ores of the Huangshan East deposit and obtained a Re–Os isochron age of 282 ± 20 Ma for the deposit. These isotopic data indicate that the rock- and ore-forming events of the main Cu–Ni sulfide deposits in northern Xinjiang occurred between the Upper Carboniferous and Lower Permian.

Rui et al. (2002b) obtained a Re–Os isochron age of 323 ± 2.3 Ma for molybdenites from the Tuwu porphyry Cu deposit. They also obtained SHRIMP U–Pb zircon ages of 308 ± 6.1 and 344.3 ± 6.8 Ma for mineralized basic volcanic rocks. Qin (2000) used K–Ar and $^{40}Ar/^{39}Ar$ methods to determine the ages of sericite and quartz from the Tuwu and Yandong ore-bearing porphyries and obtained ages of 311.1 ± 4.6 and 341.2 ± 4.9 Ma, respectively. Liu et al. (2003) obtained a SHRIMP U–Pb zircon age of 333 ± 2 Ma (weighted mean age of 16 zircon grains) for an ore-bearing porphyry in the Tuwu deposit. In summary, these isotopic data suggest that the rock-forming and mineralization ages of the Tuwu deposit range between 340 and 310 Ma.

Skarn-type Cu deposits in northern Xinjiang occur in Suoerkudouke of northern Junggar, Lamasu of west Tianshan, and Weiquan of east Tianshan. Altered pyroxene andesite, altered andesite and altered andesite–porphyrite yield a whole-rock Rb–Sr isochron age of 288.3 ± 17.6 Ma (Li et al., 1998), which is comparable with the Ar–Ar age (274.04 ± 1.11 Ma) obtained for andesite in the Suoerkudouke area (Hu et al., 1993). Since andesites in the Suoerkudouke deposit formed in the Middle Devonian, the above age cannot represent the rock-forming age of the andesites but may instead reflect the age of a tectonomagmatic event in the northern Junggar area during the Lower Permian. Garnet and epidote from ores in mineralized garnet

Table 2
Geochronological data for various ore deposits related to the Upper Paleozoic stage in north Xinjiang, China

Name of deposits	Dated minerals/rocks	Dating methods	Ages/(Ma)	Data sources
Altay Shan				
Ashele Cu–Zn	Altered dacitic breccia tuff	Rb–Sr	290.8 ± 5	Li et al. (1998)
	Dacite porphyry	Rb–Sr	296 ± 10	Li et al. (1998)
	Sub-rhyolite porphyry	Rb–Sr	294 ± 38	Li et al. (1998)
	Jaspilite	Rb–Sr	378.3 ± 39	Li et al. (1998)
	Granodiorite	Rb–Sr	360 ± 11	Li et al. (1998)
Keketale Pb–Zn	Metarhyolite breccia tuff lava	Rb–Sr	358.3 ± 9.9	Li et al. (1998)
	Zircon from two-mica granite	Pb–Pb	381 ± 18	Li et al. (1998)
	Pyrite, chalcopyrite	Sm–Nd	373 ± 15	Li et al. (1998)
	Disseminated sphalerite	Rb–Sr	273.6 ± 7.5	Li et al. (1998)
Kalatongke Cu–Ni	Cu–Ni ores	Sm–Nd isochron	281.4 ± 11.9	Li et al. (1998)
	Biotite norite	SHRIMP zircon U–Pb	287 ± 5	Han et al. (2004)
	Sulfides	Re–Os isochron	305 ± 15	This study
	Olivine norite of No.1 intrusion	Rb–Sr isochron	285 ± 17	Wang and Zhao (1991)
	Norite of No.1 intrusion	Rb–Sr isochron	298 ± 23	Wang and Zhao (1991)
	Hybrid norite of No.1 intrusion	Rb–Sr isochron	302 ± 32	Wang and Zhao (1991)
	Diabase–gabbro of No.1 intrusion	Rb–Sr isochron	317 ± 50	Wang and Zhao (1991)
Suoerkuduke skarn Cu–Mo	Altered andesite	Rb–Sr isochron	288.3 ± 17.6	Li et al. (1998)
	Garnet and epidote from skarn	Sm–Nd isochron	284.3 ± 3.9	Li et al. (1998)
Duolanasayi replacement Au	Tonalite	Single zircon U–Pb	289 ± 5	Li et al. (1998)
	Fluid inclusion of quartz vein	Rb–Sr	285 ± 43	Li et al. (1998)
	Muscovite in bearing gold ore	Ar–Ar isochron	293.1 ± 4.8	Yan et al. (2004)
	Muscovite in bearing gold ore	Ar–Ar plateau	292.8 ± 1.0	Yan et al. (2004)
Saidu replacement Au	Biotite–granite	Rb–Sr isochron	276 ± 21	Li et al. (1998)
	Fluid inclusion of quartz vein	Rb–Sr isochron	272 ± 19	Li et al. (1998)
	Fluid inclusion of quartz vein	Rb–Sr	294 ± 14	Li et al. (1998)
	Fluid inclusion of quartz vein	Rb–Sr	305.6 ± 7	Li et al. (1998)
	Biotite plagioclase granite	Rb–Sr	276 ± 21	Li et al. (1998)
	Sericite in bearing gold ore	Ar–Ar isochron	291.3 ± 8.4	Yan et al. (2004)
	Sericite in bearing gold ore	Ar–Ar plateau	289.2 ± 3.1	Yan et al. (2004)
Saerbulake Au	Arsenopyrite	Pb–Pb isochron	304.1 ± 7.4	Li et al. (1998)
	Fluid inclusion of quartz vein	Rb–Sr isochron	285 ± 43	Li et al. (1998)
	Arsenopyrite	Pb–Pb	304.1 ± 7.4	Li et al. (1998)
East Tianshan				
Huangshandong Cu–Ni	Cu–Ni sulfide ores	Re–Os isochron	282 ± 20	Mao et al. (2003)
	Ultrabasic–basic complex	Sm–Nd isochron	320 ± 38	Li et al. (1998)
	Cu–Ni sulfide ores	Sm–Nd isochron	314 ± 14	Li et al. (1998)
Huangshan Cu–Ni	Olivine norite	SHRIMP zircon U–Pb	274 ± 3	Han et al. (2004)
	Ultrabasic–basic complex	Sm–Nd isochron	308.9 ± 10.7	Li et al. (1998)
	Cu–Ni sulfide ores	Sm–Nd isochron	305.4 ± 2.4	Li et al. (1998)
Xiangshan	Gabbro	Zircon U–Pb	285 ± 1.2	Qin et al. (2002)
Tuwu Cu–Au	Volcanic rocks	Zircon U–Pb	416–361	Rui et al. (2002a,b)
	Plagiogranite porphyry	Zircon U–Pb	358–367	Rui et al. (2002a,b)
	Molybdenite	Re–Os isochron	322.7 ± 3	Rui et al. (2002a,b)
Yandong Cu–Ag	Plagiogranite porphyry	Zircon U–Pb	356 ± 8	Qin et al. (2002)
	Quartz	Ar–Ar	347.3 ± 2.1	Qin et al. (2002)
	Sericite	K–Ar	341.2 ± 4.9	Qin et al. (2002)
	Molybdenite	Re–Os isochron	343 ± 26	Zhang et al. (2004)
Kanggur replacement Au	Early stage gold ore	Rb–Sr isochron	290 ± 7.2–282 ± 5	Li et al. (1998)
	Late stage gold ore	Rb–Sr isochron	254 ± 7	Li et al. (1998)

Table 2 (*continued*)

Name of deposits	Dated minerals/rocks	Dating methods	Ages/(Ma)	Data sources
East Tianshan				
Shiyingtan epithermal Au	Quartz fluid inclusion	Rb–Sr isochron	288 ± 7–244 ± 9	Li et al. (1998)
	Andesite	Rb–Sr isochron	285 ± 12	Li et al. (1998)
	Granite porphyry	Rb–Sr isochron	266 ± 3	Li et al. (1998)
	Cryptoexplosion breccia	Rb–Sr isochron	261.6 ± 7	Li et al. (1998)
	Rhyolite tuff	Rb–Sr isochron	256.8 ± 13	Li et al. (1998)
	Quartz, orebody I	Rb–Sr isochron	288 ± 7	Li et al. (1998)
	Quartz, orebody II	Rb–Sr isochron	276 ± 7	Li et al. (1998)
	Quartz, orebody III	Rb–Sr isochron	244 ± 9	Li et al. (1998)
Xiangshan Cu–Ni	Norite–gabbro	Single zircon U–Pb	285 ± 1.2	Qin (2000)
Huangshan Cu–Ni	Olivine norite	SHRIMP zircon U–Pb	274 ± 3	Han et al. (2004)
Weiquan skarn Ag–Cu	Amphibole in skarn	^{40}Ar–^{39}Ar plateau	275.8 ± 2.87	Mao et al. (2005)
Xifengshan replacement Au	Fluid inclusion of quartz vein	Rb–Sr isochron	272 ± 3	Li et al. (1998)
Sanchakou Cu	Plagiogranite porphyry	SHRIMP zircon U–Pb	278 ± 4	Li et al. (2004)

skarns and epidote skarns yield an Sm–Nd isochron age of 284.3 ± 3.9 Ma (Li et al., 1998), suggesting that the deposit formed in Lower Permian time. Mao et al. (2002) obtained a hornblende Ar/Ar isochron age of 275.8 ± 2.8 Ma from a mineralized diorite in the Weiquan Cu–Ag deposit, which also suggests a Lower Permian age for deposit formation.

4.2. Metallogenic geodynamic mechanism for Paleozoic Cu deposits in northern Xinjiang

Northern Xinjiang is the product of a long-lived period of typical accretionary orogenic system, similar to the Cordilleran-style orogen of western North America (Goldfarb et al., 2003; Xiao et al., 2004a,b). It is characterized by a diverse and complex metallogenic history reflecting pre-, syn-, and post-accretionary tectonic events within the various lithotectonic terranes that now compose the NW corner of north Xinjiang. In the Lower to Middle Paleozoic, its continental growth was characterized by development along the margins of the amalgamated Southern Angaran and northern Tarim Blocks (Coleman, 1989; Carroll et al., 1995; Şengör et al., 1993, 1996; Jahn et al., 2004; Xiao et al., 2004a,b). The tectonic setting of northern Xinjiang is controversial, with most workers suggesting that the Paleozoic tectonic is characterized by convergence and amalgamation of terranes separated by intervening ocean basins (Coleman, 1989; Xiao et al., 1992), whereas Şengör et al. (1993, 1996) suggested that the Paleozoic geological evolution is characterized by a continuous series of accretionary events onto a unified east European–Siberian continent, with a single magmatic arc over a seawardly migrating subduction zone. Recently, Xiao et al. (2004a,b) have proposed a multiple accretionary orogenic model. Thus, the Paleozoic tectonic evolution of northern Xinjiang is not unanimously agreed and needs to be reevaluated. Geological data for the Cu province in northern Xinjiang enable us to propose the following preliminary metallogenic geodynamic mechanism.

4.2.1. Metallogenic geodynamic mechanism in northern Xinjiang, southern Altay

The southern Altay Shan is a part of the Palaeo–Asiatic orogenic belt and connects the Altay and eastern Junggar belts of China with Altay belt in Mongolia (Xiao et al., 2004b). Its geodynamic evolution is closely related to that of neighboring Kazakstan to the northwest and Mongolia to the northeast (Goldfarb et al., 2003). The Irtysh fault is the most prominent of the terrane-bounding fault in the Altay and extends for more than 1000 km into adjacent Kazakhstan and Mongolia (Goldfarb et al., 2003). It features 10-km-wide mylonites, experienced at least 1000 km of sinistral strike–slip and is well dated at (mainly) 290–280 Ma (Travin et al., 2001; Laurent-Charvet et al., 2002). The Irtysh suture zone (fault) marks a major boundary between the accretionary processes to north and south (Xiao et al., 2004b). Based on the geochronological data, the related ore deposits within the Altay Shan are recognized to belong to two age groups, i.e., VMS systems that formed between 380 and 360 Ma

and the important magmatic Cu–Ni deposits that formed at 320–290 Ma. These two age groups are considered to correspond to periods of subduction and post-collisional tectonism, respectively.

The VMS deposits known in the south Altay Shan are located between the Irtysh and Abagong faults. Such deposits are quite common in accreted arcs within Phanerozoic Cordilleran-style orogens and are well known from the accreted terranes in both California and southern Alaska (Goldfarb et al., 2003). Li et al. (1998) reported ages for the Ashele deposit that range from 373 to 255 Ma. Sm–Nd and Rb–Sr dates on volcanic rocks are 372.7 ± 14.3 and 378.3 ± 39 Ma, respectively, which are roughly the same as the stratigraphic age (Middle Devonian) of the Ashele Formation (Goldfarb et al., 2003). Li et al. (1998) obtained the dates of Rb–Sr age of 364 ± 15Ma on ores, a Sm–Nd age of 359.9 ± 11 Ma on spilite, a Rb–Sr age of 360 ± 11 Ma on granodiorite at the Ashele mine. Such data are fully consistent with the Sm–Nd age of 373 ± 15 Ma for ores from the Keketale deposit (Li et al., 1998). We can conclude that these VMS deposits formed in an interval from 380 to 360 Ma.

In the southern Altay, southwestern-directed roll-back and associated slab-detachment occurred during the Devonian (400–370 Ma) in response to later collision at the accreting continetal margin (Xiao et al., 2004b). Mafic and alkaline igneous activity, associated with formation of different types of ore deposits, took place during back arc extension (Wang, 1996), which is possibly associated with slab rollback and upwelling of the asthenosphere (Fig. 3B). Rollback also provided the heat engine for the melting associated with felsic magmatism in the Middle Devonian. The upwelling of asthenosphere also provided the heat engine of the hydrothermal fluids associated with VMS Cu–Pb–Zn mineralization (Fig. 3B). It is a process analogous to the Pliocene tectonic setting in Fiji following collision of the Ontong Java Plateau with the Melanesian arc (Squire and Miller, 2003).

The northern margin of east Junggar underwent post-collisional extension in the Upper Carboniferous–Lower Permian. The post-collisional mafic–ultramafic and granitic stocks are widely exposed throughout the southern Altay Shan and adjacent northern margin of east Junggar. They are composed of diabase–gabbro, olivine–norite, hornblende–norite, granodiorite, monzonite, K-feldspar granite, and alkaline gabbro plutons, as well as an abundance of dikes. The most widespread ages of magmatism range from 300 to 280 Ma (Hong et al., 2003). Contemporary to post-collisional magmatic activity, development of the large-scale Irtys shear zone took place. This shear zone hosts a number of orogenic gold deposits, such as Duonalasayi and Saidu. These orogenic gold deposits formed between the Upper Carboniferous and Lower Permian (Goldfarb et al., 2003; Table 2). The post-collisional extension stage also resulted in widespread emplacement of anatectic granites and the associated formation of Cu–Mo skarn deposits (e.g., the Suoerkuduk Cu–Mo deposit) (Fig. 3E). The magmatic Cu–Ni sulfide deposits, Cu–Mo skarns and orogenic gold deposits all have similar ages and are all related to the final stages of terrane collision and related post-collisional magmatism (Goldfarb et al., 2003).

Fig. 3. Schematic diagrams showing the Upper Paleozoic evolution and formation of Cu-deposits in north Xinjiang. A. From Upper Ordovician to Silurian, southern Angara developed as an active margin that faced the Zaisan Ocean (now the southern part of the Altay Moutains). Northward subduction of the Zaisan Ocean crust gave rise to the Altai–Fuyun island arc, the coeval Turgen accretionary wedge and Abagong forearc basin. Meanwhile northern subduction of Kalamaili Ocean was responsible for the Dulate–Baytag arc. B. During the Lower Devonian to Mid-Carboniferous, Zaisan Ocean lithosphere in the subducting slab has been cold enough to promote roll-back of the slab and slab detachment. The additional interaction with the rollback and slab-detachment caused accelerated back-arc extension. Cold mantle lithosphere is replaced by hot mantle asthenosphere and allows upwelling of asthenosphere, which may induce asthenosphere-dominated magmatism and associated VMS deposits (e.g., Ashele and Keketale). C. Between the Uppermost Devonian to Lower Carboniferous, southern subduction of Kalamaili Ocean slab caused the Harlike arc, whereas northward subduction of the north Tianshan Ocean was responsible for the Dananhu arc and associated with porphyry Cu–Mo–Au–Ag deposits (e.g., Tuwu). Northward subduction of the Kumishi Ocean against the Tarim block gave rise to the central Tianshan arc. D. By the Middle to Upper Carboniferous, the early Kalamaili oceanic crust was generated with a Kalamaili suture zone and the Dananhu arc system was attached to the Angaran margin, resulting in lateral growth of the Angaran continent. The magmatic front migrated southwards forming the Yamansu forearc (Xiao et al., 2004a). E. In the Uppermost Carboniferous to Lower Permian, subduction and collision ceased in the Lower Permian. Following the collisional event, an extensional event occurred in the north Xinjiang and produced voluminous ultrafic–mafic and anatectic granitoid rocks (Hong et al., 2003). These led to the formation of Cu–Ni sulfide deposits (e.g., Kalatongke and Huangshandong), skarn Cu–Mo (e.g., Suoerkudouke) and Cu–Ag (e.g., Weiquan) deposits (Han and Zhao, 2003).

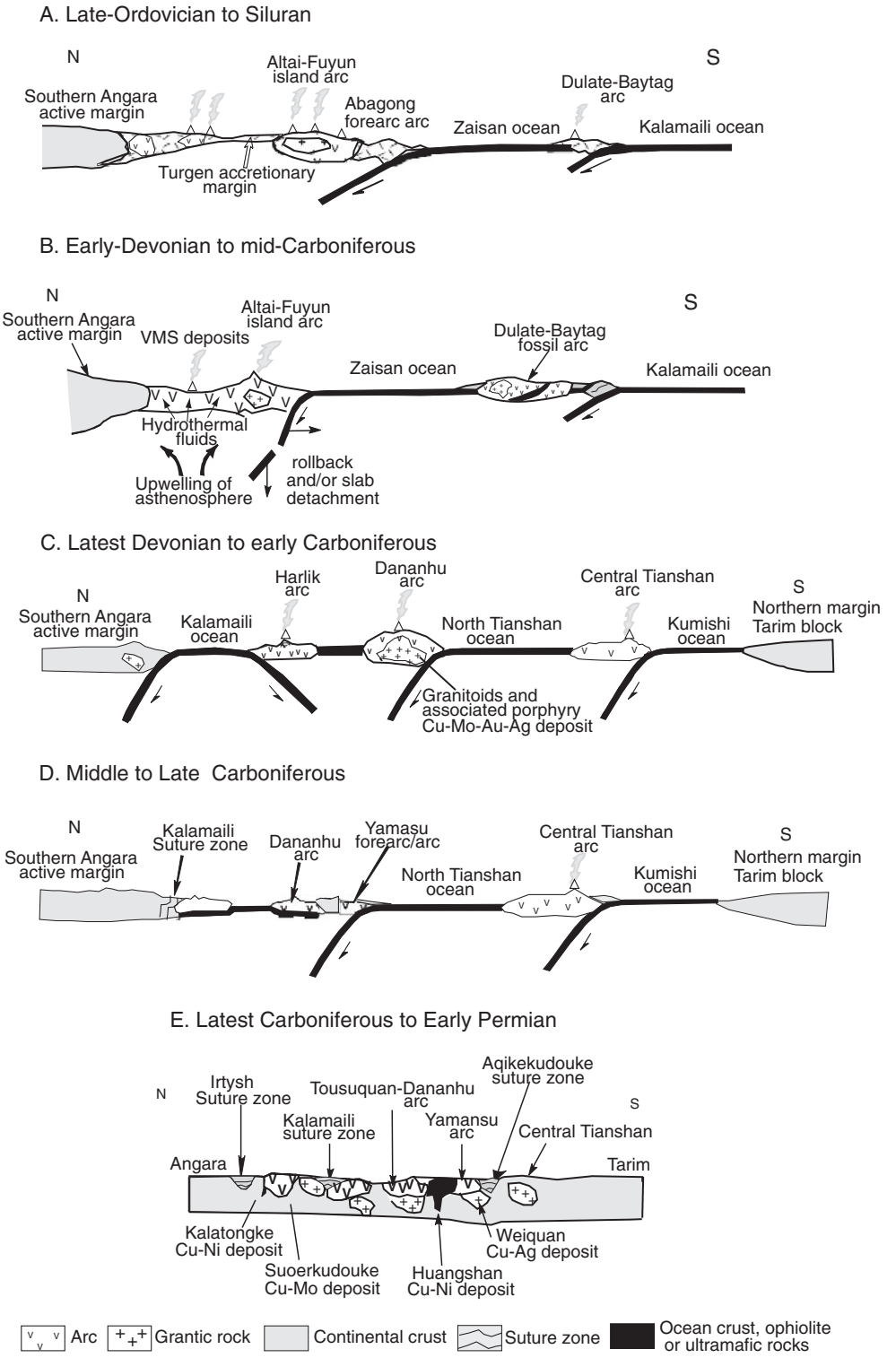
A. Late-Ordovician to Siluran
N
S
Altai-Fuyun island arc
Southern Angara active margin
Abagong forearc arc
Dulate-Baytag arc
Zaisan ocean
Kalamaili ocean
Turgen accretionary margin
B. Early-Devonian to mid-Carboniferous
N
S
Southern Angara active margin
VMS deposits
Altai-Fuyun island arc
Dulate-Baytag fossil arc
Zaisan ocean
Kalamaili ocean
Hydrothermal fluids
Upwelling of asthenosphere
rollback and/or slab detachment
C. Latest Devonian to early Carboniferous
N
S
Southern Angara active margin
Kalamaili ocean
Harlik arc
Dananhu arc
North Tianshan ocean
Central Tianshan arc
Kumishi ocean
Northern margin Tarim block
Granitoids and associated porphyry Cu-Mo-Au-Ag deposit
D. Middle to Late Carboniferous
N
S
Southern Angara active margin
Kalamaili Suture zone
Dananhu arc
Yamasu forearc/arc
North Tianshan ocean
Central Tianshan arc
Kumishi ocean
Northern margin Tarim block
E. Latest Carboniferous to Early Permian
N
S
Irtysh Suture zone
Tousuquan-Dananhu arc
Aqikekudouke suture zone
Kalamaili suture zone
Yamansu arc
Central Tianshan
Angara
Tarim
Kalatongke Cu-Ni deposit
Suoerkudouke Cu-Mo deposit
Huangshan Cu-Ni deposit
Weiquan Cu-Ag deposit
Arc
Grantic rock
Continental crust
Suture zone
Ocean crust, ophiolite or ultramafic rocks

4.2.2. Metallogenic geodynamic mechanism in east Tianshan

The Chinese eastern Tianshan is the easternmost segment of the Tianshan Mountain range in the southern Altaids, which extends eastwards through the Beishan orogenic belt to Inner Mongolia and occupies a key position between the central Asian belts to the west and east (Xiao et al., 2004a). Its geodynamic evolution is closely associated with the evolution of an ancient Tianshan Ocean between the Tarim Block and Angarann Paleozoic active margin of the CAOB (Han and Zhao, 2003; Xiao et al., 2004a). The north Tianshan ophiolitic zone was the terminal suture zone of the CAOB in the Lower Permian. It triggered the destruction of the Tianshan Ocean and the collision of the accreted Angarann continental margin with the Tarim Block (Xiao et al., 2004a), leading to the formation of the Tianshan orogen (Han and Zhao, 2003). Based on the tectonic evolution and geochronological data for the metallogenic events (Table 2), syn- and post-collisional Cu mineralization in the east Tianshan are recognized to belong to two age groups, i.e., porphyry Cu systems that formed at ca. 340–320 Ma and a variety of other deposits that formed at ca. 290–240 Ma (Mao et al., 2005). They are considered to correspond to periods of syn- and post-collisional tectonism, respectively.

Known porphyry Cu deposits in the east Tishan are positioned between the Kanguertag and Dacaotan Faults. The Xinjiang Bureau of Geology and Mineral Resources (1993) interpreted the segment as a Carboniferous island arc. The Devonian Dananhu and Tousuquan Formations mainly consist of calc-alkaline felsic volcanic lavas and tuffs; the Carboniferous Xiaorequanzi Formations and Dikaner Formations are mainly composed of lavas, pyroclastic rocks, greywacke, and carbonates (Xiao et al., 2004a; Mao et al., 2005). Devonian–Carboniferous tholetiitic basalt and calc-alkaline andesite were interpreted to be volcanic rocks of an island arc (Yang et al., 2000; Zhou et al., 2001). Rocks of the arc are intruded by a number of batholiths comprising diorite, granodiorite, and granite bodies (Mao et al., 2005).

Rui et al. (2002a) and Qin (2000) reported Rb–Sr isochron and single U–Pb data from host rock of the Tuwu deposit, which indicated an age range of 356–369 Ma, suggesting that they formed in the Upper Devonian and not in the Lower Carboniferous. SHRIMP zircon U–Pb ages of 383 ± 9 Ma were for an arc monzonitic granite and 357.3 ± 6.2 Ma for a granodirite from these intrusions (Song et al., 2002). The grano-porphyry related magmas at the Tuwu–Yandong were emplaced at a range from 333 ± 2 to 334 ± 2 Ma (Liu et al., 2003). These data indicate that the arc has a Middle Devonian to Lower Carboniferous age (Xiao et al., 2004a). Qin (2000) and Rui et al. (2002a) obtained a single grain U/Pb zircon age of 356 ± 8 and 361 ± 8 Ma for granite from the Yandong–Tuwu Cu mine, respectively. A Re–Os isochron date of 322.7 ± 2.3 Ma of ores from Tuwu–Yandong deposits (Rui et al., 2002a) and a $^{39}Ar/^{40}Ar$ age of 347 ± 2 Ma of sericite for altered granite–porphyry from Yandong mine were reported (Qin, 2000). This indicates that magmatism and associated porphyry Cu mineralization lasted until the end of the Lower Carboniferous. The Dananhu–Tousuquan arc formed as a result of the north-dipping subduction of the Tianshan Ocean (Fig. 3C). Following the collisional event, a post-collisional extensional event occurred in the east Tianshan during the Permian (Han and Zhao, 2003). Measured ages range from 290 to 270 Ma (Li et al., 1998; Mao et al., 2003; Table 2). The post-collisional extension stage also resulted in widespread emplacement of post-orogenic granites and the associated formation of skarn-type Ag–Cu deposits (e.g., the Weiquan Ag–Cu deposit). Development of the large-scale Kanguer ductile shear zone was probably synchronous with post-collisional magmatic activities; the shear zone hosts a number of orogenic gold deposits, such as Kanguer, Matoutan, Xifengshan and Shiyingtan (Zhang et al., 2004; Mao et al., 2005). These orogenic gold deposits formed during the Permian; ages range from 290 to 240 Ma (Table 2). It is suggested that the orogenic gold, skarn Cu–Mo and magmatic Cu–Ni sulfide deposits have similar ages. They are all products of post-collisional Upper Carboniferous to Early Permian lithospheric thinning and delamination and mantle–crust interaction driven by a mantle plume in east Tian orogenic belt (Xia et al., 2003, 2004; Zhou et al., 2004; Mao et al., 2005).

In east Tianshan, development of Upper Paleozoic Cu deposits was closely associated with the subduction and closure of the ancient Tianshan Ocean, lying between the Tarim and the Junggar Blocks (He et al., 1994; Han and Zhao, 2003; Xiao et al., 2004a,b). In Upper Devonian to Lower Carboniferous time, the

northern margin of the Tarim Craton formed a passive-type continental margin, whereas the ancient Tianshan Ocean was subducted to the north beneath the southern margin of the Junggar–Kazakhstan Block, resulting in the development of the Tousuquan–Dananhu magmatic arc and associated porphyry-type Cu–Mo–Au–Ag deposits (Fig. 3C). In the Upper Carboniferous to Lower Permian, multiple soft collisions left a suture zone represented by the north Tianshan accretion–collision complex, which includes ophiolitic fragments. In the Lower Permian, the Tianshan orogen entered into a post-collision orogenic stage, leading to the formation of the Kangguer ductile shear zone and the widespread emplacement of granitoids rocks and eruption of within-plate volcanism at 254~234 Ma, resulting in the formation of volcanic hydrothermal Cu deposits in the Dananhu–Tousuquan belt and skarn-type Cu–Ag deposits (~276Ma) in the Aqishan–Yamansu belt (Fig. 3E).

5. Conclusions

Cu–(Ni) deposits in northern Xinjiang are assigned to four major types: (1) Devonian pre-accretionary VHMS Cu–Pb–Zn deposits, (2) Lower Carboniferous syn-accretionary porphyry-type Cu–Mo–(Au) deposits, (3) Upper Carboniferous–Lower Permian syn- to post-accretionary magmatic Cu–Ni sulfide deposits; and (4) Upper Carboniferous–Lower Permian post-accretionary skarn Cu–Mo–Au–Ag deposits.

Our metallogenic–geodynamic model for the VMS deposits generally supports long-lived subduction and growth by rollback forearc accretion (Şengör et al., 1996; Xiao et al., 2004a,b), based on the forearc accretionary part of Japanese orogenesis. The Devonian forearc rollback and associated slab tearing triggered back arc extension and upwelling of the asthenosphere, which also provided the heat to mineralization fluids associated with VMS Cu–Pb–Zn mineralization.

During the Upper Devonian to Lower Carboniferous, north-dipping subduction beneath the Dananhu–Harlic arc led to the development of syn-accretion porphyry Cu deposits. From Upper Carboniferous to Lower Permian, syn- to post-accretionary Cu and Ni deposits developed in association with a series of convergent events, which were then followed by a post-collisional extension event, leading to emplacement of intrusions and the formation of the skarn and volcanic–hydrothermal Cu deposits in northern Xinjiang in Lower Permian time.

Acknowledgements

This paper benefited greatly from the many achievements of the Xinjiang Bureau of Geology and Mineral resources and the National 305 Project. We are indebted to Bin Cui, Kezhang Qin, Zhaochong Zhang, Yitian Wang, Jinyi Li, Tianlin Ma, and Lianchang Zhang for discussions. Many of the ideas in this paper were initiated and rectified during these discussions. In particular, we thank Stephen E. Kesler and an anonymous *Ore Geology Reviews* reviewer for their perceptive comments, which led to substantial improvements to the paper. The careful editorial handling and cheerful encouragement by Nigel J. Cook is gratefully appreciated. This study is financially supported by the State Basic Research Program of China (2001CB409801), the National Key Project (96-915-07), and the NSFC Program (40172080). This paper forms a contribution to IGCP 473, 480, 509 and 420.

References

Allen, M.B., Vincent, S.J., 1997. Fault reactivation in the Junggar region, northwest China—the role of basement structures during Mesozoic–Cenozoic compression. Journal of the Geological Society, London 154, 151–155.

Allen, M.B., Windley, B.F., Zhang, C., 1992. Paleozoic collisional tectonics and magmatism of the Chinese Tianshan, central Asia. Tectonophysics 220, 89–115.

Allen, M.B., Windley, B.F., Zhang, C., Guo, J.H., 1993. Evolution of the Turfan basin, Chinese central Asia. Tectonics 12, 889–896.

Allen, M.B., Şengör, A.M.C., Natal'in, B.A., 1995. Junggar, Turpan and Alakol basins as Late Permian to Early Triassic extensional structures in a sinistral shear zone in the Altaid orogenic collage, central Asia. Journal of the Geological Society of London 152, 327–338.

Bureau of Geology and Mineral Resources of Xinjiang Uygur Autonomous Region, 1993. Regional Geology of Xinjiang Uygur Autonomous Region. People's Republic of China, Ministry of Geology and Mineral Resources, Geological Memoirs, Series 1, vol. 32. Geological Publishing House, Beijing. 206 pp. (in Chinese with English abstract).

Carroll, A.R., Graham, S.A., Hendrix, M.S., Ying, D., Zhou, D., 1995. Late Paleozoic tectonic amalgamation of northwestern China: sedimentary record of the northern Tarim, northwestern

Turpan, and southern Junggar basins. Geological Society of America Bulletin 107, 571–594.

Chen, Y.B., 1999 Isotope geochemistry study on the basement of the western Tianshan, Xinjiang, northwestern China. PhD thesis, Guangzhou Institute of Geochemistry, Chinese Academy of Sciences. 51 pp.

Chen, B., Jahn, B.M., 2002. Geochemical and isotopic studies of the sedimentary and granitic rocks of the Altai orogen of northwest China and their tectonic implications. Geological Magazine 139, 1–13.

Chen, B., Jahn, B.M., 2004. Genesis of post-collisional granitoids and basement nature of the Junggar terrane, NW China: Nd–Sr isotope and trace element evidence. Journal of Asian Earth Sciences 23, 691–703.

Chen, Y.C., Ye, Q.T., Feng, J., Mu, C.L., Zhou, L.R., Wang, Q.M., Huang, G.Z., Zhuang, D.Z., Ren, B.C., 1996. Ore-forming Conditions and Metallogenic Prognosis of the Ashele Copper–zinc Metallogenic Belt, Xinjiang, China. Geological Publishing House, Beijing. 330 pp. (in Chinese with English abstract).

Chen, Z.F., Cheng, S.D., Liang, Y.H., Xu, X., 1997. Opening–closing Tectonics and Mineralization in Xinjiang. Xinjiang Science Technology and Hygiene Publishing House, Urumqi. 394 pp. (in Chinese with English abstract).

Coleman, R.G., 1989. Continental growth of northern China. Tectonics 8, 621–635.

Feng, J.Z., Zeng, Y.S., Fu, S.X., 2000a. Geology, genetic types and metallogeny of gold deposits in the eastern Tianshan, Xinjiang. Acta Geologica Sinica 74, 559–564.

Feng, C.Y., Xue, C.J., Zhang, L.C., 2000b. Geochemistry of the Xitan epothermal gold–silver deposit, east Tianshan Mountains. Mineral Deposits 19, 322–329 (in Chinese with English abstract).

Gao, J., Li, M.S., Xiao, X.C., Tang, Y.Q., He, G.Q., 1998. Paleozoic tectonic evolution of the Tianshan orogen, northwestern China. Tectonophysics 287, 213–231.

Goldfarb, R.J., Mao, J.W., Seltmann, R., Wang, D.H., Xiao, W.J., Hart, C., 2003. Tectonic and metallogenic evolution of the Altay Shan, northern Xinjiang, Uygur Autonomous region, northwestern China. In: Mao, J.W., Goldfarb, R.J., Seltmann, R., Wang, D.H., Xiao, W.J., Hart, C. (Eds.), Tectonic Evolution and Metallogeny of the Chinese Altay and Tianshan. Proceedings Volume of the International Symposium of the IGCP-473 Project in Urumqi. CERCAMS/Natural History Museum, London, pp. 17–30.

Han, C.M., 2002. Research on Metallogenic Series of Copper Deposits in East Tianshan Mountains. China University of Geosciences, Beijing. 138 pp. (in Chinese with English abstract).

Han, C.M., Zhao, G.C., 2003. Major types and characteristics of the late Paleozoic ore deposits, east Tianshan, northwest China. International Geology Review 45, 798–814.

Han, C.M., Mao, J.W., Yang, J.M., 2002. Types of late Paleozoic endogenetic metal deposits and related geodynamical evolution in the east Tianshan. Acta Geologica Sinica 76, 222–234 (in Chinese with English abstract).

Han, C.M, Rui, Z.Y., Mao, J.W., Yang, J.M., Wang, Z.L., Yuan, W.M., 2003. Geological characteristics of the Tuwu copper deposit, Hami, Xinjiang. In: Mao, J.W., Goldfarb, R.J., Seltmann, R., Wang, D.H., Xiao, W.J., Hart, C. (Eds.), Tectonic Evolution and Metallogeny of the Chinese Altay and Tianshan. Proceedings Volume of the International Symposium of the IGCP-473 Project in Urumqi. CERCAMS/Natural History Museum, London, pp. 249–260.

Han, B.F., Ji, J.Q., Song, B., Chen, L.H., Li, Z.H., 2004. SHRIMP zircon U–Pb ages of Kalatongke No. 1 and Huangshandong Cu–Ni- bearing mafic–ultramafic complexes, north Xinjiang, and geological implications. Chinese Science Bulletin 49, 2324–2328 (in Chinese).

He, G.Q., Li, M.S., Liu, D.Q., Tang, Y.L., Zhou, R.H., 1994. Paleozoic Crust Evolution and Mineralization of Xinjiang, China. Xinjiang People Publishing House, Urumqi. 424 pp. (in Chinese with English abstract).

Hendrix, M.S., Graham, S.A., Carroll, A.R., 1992. Sedimentary record and climatic implications of recurrent deformation in the Tian Shan—evidence from Mesozoic strata of the north Tarim, south Junggar, and Turfan basins, northwest China. Geological Society of America Bulletin 104, 53–79.

Hong, D.W., Wang, S.G., Xie, Y.L., Zhang, J.S., Wang, T., 2003. Granitoids and related metallogeny of central Asia. In: Mao, J.W., Goldfarb, R.J., Seltmann, R., Wang, D.H., Xiao, W.J., Hart, C. (Eds.), Tectonic Evolution and Metallogeny of the Chinese Altay and Tianshan. Proceedings Volume of the International Symposium of the IGCP-473 Project in Urumqi. CERCAMS/Natural History Museum, London, pp. 75–106.

Hu, A.Q., Zhang, G.X., Li, Q.X., 1986a. Isotope geochemistry and crustal evolution of northern Xinjiang. In: Tu, A.Q. (Ed.), New Improvement of Solid Geoscience in Northern Xinjiang. Science in China Press, Beijing, pp. 27–37 (in Chinese with English abstract).

Hu, A.Q., Zhang, Z.B., Zhang, J.B., 1986b. Middle Tianshan rift zone Precambrian metamorphic basement dating and evolution of East Tianshan Mountains. Geochemistry 15, 23–25 (in Chinese with English abstract).

Hu, A.Q., Zhang, G.X., Li, Q.X., 1993. Isotope geochemistry and crustal evolution of northern Xinjiang. In: Tu, A.Q. (Ed.), New Improvement of Solid Geoscience in Northern Xinjiang. Science in China Press, Beijing, pp. 27–38 (in Chinese with English abstract).

Hu, A.Q., Jahn, B.M., Zhang, G.X., 2000. Crustal evolution and Phanerozoic crustal growth in northern Xinjiang: Nd isotopic evidence: Part I. Isotopic characterization of basement rocks. Tectonophysics 328, 15–51.

Huang, J.H., Lu, X.C., Zhu, X.N., 1995. Advance in research of the ophiolites in Hongguleleng of north Junggar, Xinjiang. Xinjiang Geology 13, 20–30 (in Chinese with English abstract).

Huang, X., Jin, C.W., Sun, B.S., Pan, J., Zhang, R.H., 1997. Study on the Armantai ophiolite, Xinjiang, by Nd–Sr isotope geology. Acta Petrologica Sinica 13, 85–91 (in Chinese with English abstract).

Jahn, B.M., Natalin's, B., Dobretsov, N., 2004. Phanerozoic continental growth in central Asia. Journal of Asian Earth Sciences 23, 599–603.

Ji, J.S., Tao, H.X., Lu, Z.R., 1994. Geological Characteristics and Mineralization of Kangguer Gold Deposit Zone in Eastern

Tianshan Mountains. Geological Publishing House, Beijing. 325 pp. (in Chinese with English abstract).

Ji, J.S., Li, H.Q., Zhang, L.C., 1999. Sm–Nd and Rb–Sr isotopical ages of magnetite–chlorite formation gold deposit in the volcanic rock area of Late Paleozoic era, east Tianshan. Chinese Science Bulletin 44, 1801–1804 (in Chinese with English abstract).

Jiang, Y.D., 1984. A preliminary approach to the basement of Junggar district. Xinjiang Geology 4, 11–16 (in Chinese with English abstract).

Laurent-Charvet, S., Charvet, J., Shu, L.S., Ma, R.S., Lu, H.F., 2002. Paleozoic late collosional strike–slip deformations in Tianshan and Altay, eastern Xinjiang, NW China. Terra Nova 14, 249–256.

Li, H., Li, X.Z., 1991. PGE-forming condition and target of exploration in Xinjiang, Bulletin of Xi'an Geological and Resource Institute. Chinese Academy of Geological Sciences 33, 1–93.

Li, X.J., Liu, W., 2002. Fluid inclusion and stable isotope constrains on the genesis of the Mazhuangshan gold deposit, eastern Tianshan Mountains of China. Acta Petrologica Sinica 18, 551–558 (in Chinese with English abstract).

Li, C.Y., Wang, Q., Liu, X.Y., Tang, Y.Q., 1982. Explanatory Notes to the Tectonic Map of Asia. Cartographic Publishing House, Beijing. 49 pp. (in Chinese with English abstract).

Li, H.Q., Xie, C.F., Chang, H.L., Cai, H., Zhu, J.P., Zhou, S., 1998. Study on Metallogenetic Chronology of Nonferrous and Precious Metallic Ore Deposits in North Xinjiang, China. Geological Publishing House, Beijing. 264 pp. (in Chinese with English abstract).

Li, H.Q., Chen, F.W., Lu, Y.F., Yang, H.M., Guo, J., Mei, Y.P., 2004. Zircon SHRIMP U–Pb age and strontium isotopes of mineralized granitoids in the Sanchakou copper molymetallic depoist, east Tianshan Mountains. Acta Geoscientica Sinica 25 (2), 191–195.

Liu, D.Q., Tang, Y.L., Zhou, R.H., 1996. Metallogenic series types of deposits in Xinjiang. Mineral Deposits 15, 207–215 (in Chinese with English abstract).

Liu, D.Q., Chen, Y.C., Wang, D.H., 2003. A discussion on problems related to mineralization of Tuwu–Yandong Cu–Mo ore field in Hami, Xinjiang. Mineral Deposits 22, 334–344 (in Chinese with English abstract).

Lu, Q.X., Liu, X.F., 1989. Study of geochronology for Sn-bearing granite belt from the east Junggar in Xinjiang. The Compilation for Fourth Chinese Isotopic Geochronology and Geochemistry Symposium, pp. 3–4 (in Chinese).

Ma, R.S., Shu, L.S., Sun, J.Q., 1997. Tectonic Framework and Crust Evolution of Eastern Tianshan Mountains. Geological Publishing House, Beijing. 202 pp. (in Chinese with English abstract).

Mao, J.W., Yang, J.M., Qu, W.J., 2002. Re–Os dating of Cu–Ni sulfide ores from Huangshandong deposit in Xinjiang and its geological significance. Mineral Deposits 21, 330–339 (in Chinese with English abstract).

Mao, J.W., Yang, J.M., Qu, W.J., 2003. Re–Os age of Cu–Ni ores from the Huangshandong Cu–Ni sulfide deposit in the east Tianshan Mountains and its implication for geodynamic processes. Acta Geologica Sinica 77, 220–226.

Mao, J.W, Goldfarb, R.J., Wang, Y.T., Hart, C.J.R., Wang, Z.L., Yang, J.M., 2005. Late Paleozoic base and precious metal deposits, east Tianshan, Xinjiang, China: characteristics and geodynamic setting. Episodes 28, 1–14.

Pirajno, F., Luo, Z.Q., Liu, S.F., Dong, L.H., 1997. Gold deposits in the eastern Tianshan, northwestern China. International Geology Review 39, 891–904.

Qin, K.Z., 2000 Metallogenesis in relation to central-Asia style orogeny of northern Xinjiang. Institute of Geology and Geophysics, Chinese Academy of Science, Beijing, Unpublished Postdoctoral Research Report. 230 pp. (in Chinese with English abstract).

Qin, K.Z., Sun, S., Li, J.L., 2002. Paleozoic epithermal Au and porphyry Cu deposits in north Xinjiang, China: epochs, features, tectonic linkage and exploration significance. Resource Geology 52, 291–300.

Ren, J.S., Jiang, C.F., 1980. Tectonics and the Evolution of China. Science Press, Beijing. 124 pp. (in Chinese with English abstract).

Rui, Z.Y., Wang, F.T., Li, H.H., 2001. New advance of porphyry copper deposits in eastern Tianshan Mountains, Xinjiang. Chinese Geology 28, 11–17 (in Chinese with English abstract).

Rui, Z.Y., Wang, L.S., Wang, Y.T., 2002a. Discussion on matallogenic epoch of Tuwu and Yandong porphyry copper deposits in eastern Tianshan Mountains, Xinjiang. Mineral Deposits 21, 16–22 (in Chinese with English abstract).

Rui, Z.Y., Goldfarb, R.J., Qiu, Y.M., Zhou, T.H., Pirajno, F., Yun, G., 2002b. Paleozoic–early Mesozoic gold deposits of the Xinjiang Autonomous Region, northwestern China. Mineralium Deposita 37, 393–418.

Şengör, A.M.C., Natal'in, B.A., Burtman, V.S., 1993. Evolution of the Altaids collage and Paleozoic crustal growth in Eurasia. Nature 364, 299–307.

Şengör, A.M.C., Natal'in, B.A., Burtman, V.S., 1996. Turkic-type orogeny and its role in the making of the continental crust. Annual Review of Earth and Planetary Sciences 24, 263–337.

Shen, Y.C., Xiao, Z., Lin, H., 1996. The characteristics of the Altay–Junggar gold mineralization belt. In: Jin, C. (Ed.), Geology of Main Gold Metallogenic Belts in Northern Part of China. Seismological Press, Beijing, pp. 7–31 (in Chinese with English abstract).

Song, B., Li, J.Y., Li, W.Q., Wang, K.Z., Wang, Y., 2002. SHRIMP dating of zircon from Dananhu and Keziekalasai granitoid bothlith in southern margin of Tuha basin, east Tianshan, NW China and their geological implication. Xinjiang Geology 20 (4), 342–345 (in Chinese with English abstract).

Squire, R.J., Miller, J.M.L., 2003. Synchronous compression and extension in east Gondwana: tectonic controls on world-class gold deposits at 440 Ma. Geology 31, 1073–1076.

Travin, A.V., Boven, A., Plotnikov, A.V., Vladimirov, V.G., Theunissen, K., Vladimirov, A.G., Melnikov, A.I., Titov, A.V., 2001. $^{40}Ar/^{39}Ar$ dating of ductive deformationas in the Irtysh shear zone eastern Kazakhstan. Geochemistry International 39, 1237–1241.

Wang, H.Z., 1986. Atlas of Paleogeography of China. Cartographic Publishing House, Beijing. 80 pp. (in Chinese with English abstract).

Wang, D.H., 1996. The volcanic rocks and mineralization in Ashele Cu mine, Xinjiang. Scientia Geologica Sinica 31, 163–169 (in Chinese with English abstract).

Wang, R.M., Zhao, C.L., 1991. Kalatongke Copper–Nickel Sulfide No.1 Ore Deposits in Xinjiang. Geological Publishing House, Beijing. 391pp. (in Chinese with English abstract).

Wang, J.B., Qin, K.Z., Wu, Z.L., Hu, J.H., Deng, J.N., 1998. Volcanic Exhalative Sedimentary Lead–Zinc Deposits in the South Margin of Altay Mountains, Xinjiang. Geological Publishing House, Beijing. 210 pp. (in Chinese with English abstract).

Wang, F.T., Feng, J., Hu, J.W., 2001a. Characteristics and significance of the Tuwu porphyry copper deposit, Xinjiang. Chinese Geology 28, 36–39 (in Chinese with English abstract).

Wang, F.T., Zhuang, D.Z., Hu, J.W., 2001b. Application of geophysical exploration method in the Tuwu area, Xinjiang—on the prospecting model of porphyry copper deposits. Chinese Geology 28, 40–46 (in Chinese with English abstract).

Wang, D.H., Chen, Y.C., Xu, Z.G., Li, T.D., Fu, X.J., 2002. Minernogenetic Series of Mineral Deposits and Regularity of Mineralization in the Altaid Metallogenic Province, Xinjiang, China. Atomic Energy Press, Beijing. 498 pp. (in Chinese).

Watson, M.P., Hayward, A.B., Parkinson, D.M., Zhang, Z.M., 1987. Block tectonic history, basin development and petroleum source rock deposition onshore China. Marine and Petroleum Geology 4, 205–225.

Windley, B.F., Allen, M.B., Zhang, C., Zhao, Z.Y., Wang, G.R., 1990. Paleozoic accretion and Cenozoic redeformation of the Chinese Tien Shan Range, central Asia. Geology 18, 128–131.

Windley, B.F., Kröner, A., Guo, J., Qu, G., Li, Y., Zhang, C., 2002. Neoproterozoic to Paleozoic geology of the Altai orogen, NW China: new zircon age data and tectonic evolution. Journal of Geology 110, 719–739.

Xia, L.Q., Xu, X.Y., Xia, Z.C., Li, X.M., Ma, Z.P., Wang, L.S., 2003. Carboniferous post-collisional rift volcanism of the Tianshan Mountains, northwestern China. Acta Geologica Sinica 77 (3), 338–360.

Xia, L.Q., Xu, X.Y., Xia, Z.C., Li, X.M., Ma, Z.P., Wang, L.S., 2004. Petrogenesis of Carboniferous rift-related volcanic rocks in the Tianshan, northwestern China. Geological Society of America Bulletin 116, 419–433.

Xiao, X.C., Tang, Y.Q., Feng, Y.M., 1992. Tectonics Evolution of Northern Xinjiang and Its Adjacent Regions. Geological Publishing House, Beijing. 169 pp. (in Chinese with English abstract).

Xiao, W.J., Zhang, L.C., Qin, K.Z., Sun, S., Li, J.L., 2004a. Paleozoic accretionary and collisional tectonics of the eastern Tianshan (China): implications for the continental growth of central Asia. American Journal of Science 304, 370–395.

Xiao, W.J., Windley, B.F., Badarch, G., Sun, S., Li, J.L., Qin, K.Z., Wang, Z.H., 2004b. Palaeozoic accretionary and convergent tectonics of the southern Altaids: implications for the lateral growth of central Asia. Journal of the Geological Society of London 161, 339–342.

Yan, S.H., Zhang, Z.C., Wang, D.H., Chen, B.L., He, L.X., Zhou, G., 2003. Kalatongke magmatic copper–nickel sulfide deposit. In: Mao, J.W., Goldfarb, R.J., Seltmann, R., Wang, D.H., Xiao, W.J., Hart, C. (Eds.), Tectonic Evolution and Metallogeny of the Chinese Altay and Tianshan. Proceedings Volume of the International Symposium of the IGCP-473 Project in Urumqi. CERCAMS/Natural History Museum, London, pp. 131–151.

Yan, S.H., Chen, W., Wang, Y.T., Zhang, Z.C., Chen, B.L., 2004. $^{40}Ar/^{39}Ar$ dating and its significance of the Ertix gold metallogenic belt in the Altay orogen, Xinjiang. Acta Geologica Sinica 78 (4), 500–506.

Yang, X.K., Cheng, H.B., Ji, J.S., Luo, G.C., Tao, H.X., 2000. Analysis on gold and copper ore-forming setting with ore-forming system of eastern Tianshan. Journal of Xi'an Engineering University 22, 7–14 (in Chinese with English abstract).

Zhang, C., Huang, X., 1992. Age and tectonic settings of ophiolites in western Junggar, Xinjiang. Geology Reviews 38, 509–524 (in Chinese with English abstract).

Zhang, L.C., Ji, J.S., Li, H.Q., 2000. The geochemical features and source of two-type ore-forming fluids in Kangguer gold ore belt, east Tianshan Mountains. Acta Petrologica Sinica 16, 535–541 (in Chinese with English abstract).

Zhang, L.C., Liu, T.B., Shen, Y.C., Li, G.M., Ji, J.S., 2002. Isotopic geochronology of the Late Paleozoic Kangurtag gold deposit of east Tianshan Mountain, Xinjiang, NW China. Resource Geology 52, 249–261.

Zhang, L.C., Shen, Y.C., Ji, J.S., 2003. Characteristics and genesis of Kanggur gold deposit in the eastern Tianshan mountains, NW China: evidence from geology, isotope distribution and chronology. Ore Geology Reviews 23, 71–90.

Zhang, L.C., Xiao, W.J., Qin, K.Z., Ji, J.S., Yang, X.K., 2004. Types, geological features and geodynamic significances of gold–copper deposits in the Kanggurtag metallogenic belt, eastern Tianshan, NW China. International Journal of Earth Sciences 93, 224–240.

Zhou, L.R., 1989. Zircon geochronology of granitoids and its implication for geology in the west Junggar of Xinjiang, China. Northwest Geology 6, 30–31 (in Chinese with English abstract).

Zhou, J.Y., Cui, B.F., Xiao, H.L., Chen, S.Z., Zhu, D.M., 2001. The Kangguertag–Huangshan collision zone of bilateral subduction and its metallogenic model and prognosis in Xinjiang, China. Volcanology and Mineral Resources 22, 252–263 (in Chinese with English abstract).

Zhou, M.F., Lesher, C.M., Yang, Z.X., Li, J.W., Sun, M., 2004. Geochemistry and petrogenesis of 270 Ma Ni–Cu–(PGE) sulfide-bearing mafic intrusions in the Huangshan district, eastern Xinjiang, northwest China: implications for the tectonic evolution of the central Asian orogenic belt. Chemical Geology 209, 233–257.